doi:10.1038/nature25738

The Beaker phenomenon and the genomic transformation of northwest Europe

A list of authors and their affiliations appears at the end of the paper.

From around 2750 to 2500 BC, Bell Beaker pottery became widespread across western and central Europe, before it disappeared between 2200 and 1800 BC. The forces that propelled its expansion are a matter of long-standing debate, and there is support for both cultural diffusion and migration having a role in this process. Here we present genome-wide data from 400 Neolithic, Copper Age and Bronze Age Europeans, including 226 individuals associated with Beaker-complex artefacts. We detected limited genetic affinity between Beaker-complex-associated individuals from Iberia and central Europe, and thus exclude migration as an important mechanism of spread between these two regions. However, migration had a key role in the further dissemination of the Beaker complex. We document this phenomenon most clearly in Britain, where the spread of the Beaker complex introduced high levels of steppe-related ancestry and was associated with the replacement of approximately 90% of Britain's gene pool within a few hundred years, continuing the east-to-west expansion that had brought steppe-related ancestry into central and northern Europe over the previous centuries.

During the third millennium BC, two new archaeological pottery styles expanded across Europe and replaced many of the more localized styles that had preceded them[1]. The expansion of the 'Corded Ware complex' in north-central and northeastern Europe was associated with people who derived most of their ancestry from populations related to Early Bronze Age Yamnaya pastoralists from the Eurasian steppe[2–4] (henceforth referred to as 'steppe'). In western Europe there was the equally expansive 'Bell Beaker complex', defined by assemblages of grave goods that included stylized bell-shaped pots, copper daggers, arrowheads, stone wristguards and V-perforated buttons[5] (Extended Data Fig. 1). The oldest radiocarbon dates associated with Beaker pottery are from around 2750 BC in Atlantic Iberia[6], which has been interpreted as evidence that the Beaker complex originated in this region. However, the geographic origins of this complex are still debated[7] and other scenarios—including an origin in the Lower Rhine area, or even multiple independent origins—are possible (Supplementary Information section 1). Regardless of geographic origin, by 2500 BC the Beaker complex had spread throughout western Europe and northwest Africa and had reached southern and Atlantic France, Italy and central Europe[5], where it overlapped geographically with the Corded Ware complex. Within another hundred years, it had expanded to Britain and Ireland[8]. A major debate in archaeology has revolved around the question of whether the spread of the Beaker complex was mediated by the movement of people, culture or a combination of both[9]. Genome-wide data have revealed high proportions of steppe-related ancestry in Beaker-complex-associated individuals from Germany and the Czech Republic[2–4], which shows that these individuals derived from mixtures of populations from the steppe and the preceding Neolithic farmers of Europe. However, a deeper understanding of the ancestry of people associated with the Beaker complex requires genomic characterization of individuals across the geographic range and temporal duration of this archaeological phenomenon.

Ancient DNA data

To understand the genetic structure of ancient people associated with the Beaker complex and their relationship to preceding, subsequent and contemporary peoples, we used hybridization DNA capture[4,10] to enrich ancient DNA libraries for sequences overlapping 1,233,013 single nucleotide polymorphisms (SNPs), and generated new sequence data from 400 ancient Europeans dated to between approximately 4700 and 800 BC, excavated from 136 different sites (Extended Data Tables 1, 2; Supplementary Table 1; Supplementary Information section 2). This dataset includes 226 Beaker-complex-associated individuals from Iberia ($n = 37$), southern France ($n = 4$), northern Italy ($n = 3$), Sicily ($n = 3$), central Europe ($n = 133$), the Netherlands ($n = 9$) and Britain ($n = 37$), and 174 individuals from other ancient populations, including 118 individuals from Britain who lived both before ($n = 51$) and after ($n = 67$) the arrival of the Beaker complex (Fig. 1a, b). For genome-wide analyses, we filtered out first-degree relatives and individuals with low coverage (fewer than 10,000 SNPs) or evidence of DNA contamination (Methods) and combined our data with previously published ancient DNA data (Extended Data Fig. 2) to form a dataset of 683 ancient samples (Supplementary Table 1). We merged these data with those from 2,572 present-day individuals genotyped on the Affymetrix Human Origins array[11,12] as well as with 300 high-coverage genomes[13]. To facilitate the interpretation of our genetic results, we also generated 111 direct radiocarbon dates (Extended Data Table 3; Supplementary Information section 3).

Y-chromosome analysis

The Y-chromosome composition of Beaker-complex-associated males was dominated by R1b-M269 (Supplementary Table 4), which is a lineage associated with the arrival of steppe migrants in central Europe after 3000 BC[2,3]. Outside Iberia, this lineage was present in 84 out of 90 analysed males. For individuals for whom we determined the R1b-M269 subtype ($n = 60$), we found that all but two had the derived allele for the R1b-S116/P312 polymorphism, which defines the dominant subtype in western Europe today[14]. By contrast, Beaker-complex-associated individuals from the Iberian Peninsula carried a higher proportion of Y haplogroups known to be common across Europe during the earlier Neolithic period[2,4,15,16], such as I ($n = 5$) and G2 ($n = 1$); R1b-M269 was found in four individuals with a genome-wide signal of steppe-related ancestry, and of these, the two with higher coverage could be classified

A list of authors and their affiliations appears at the end of the paper.

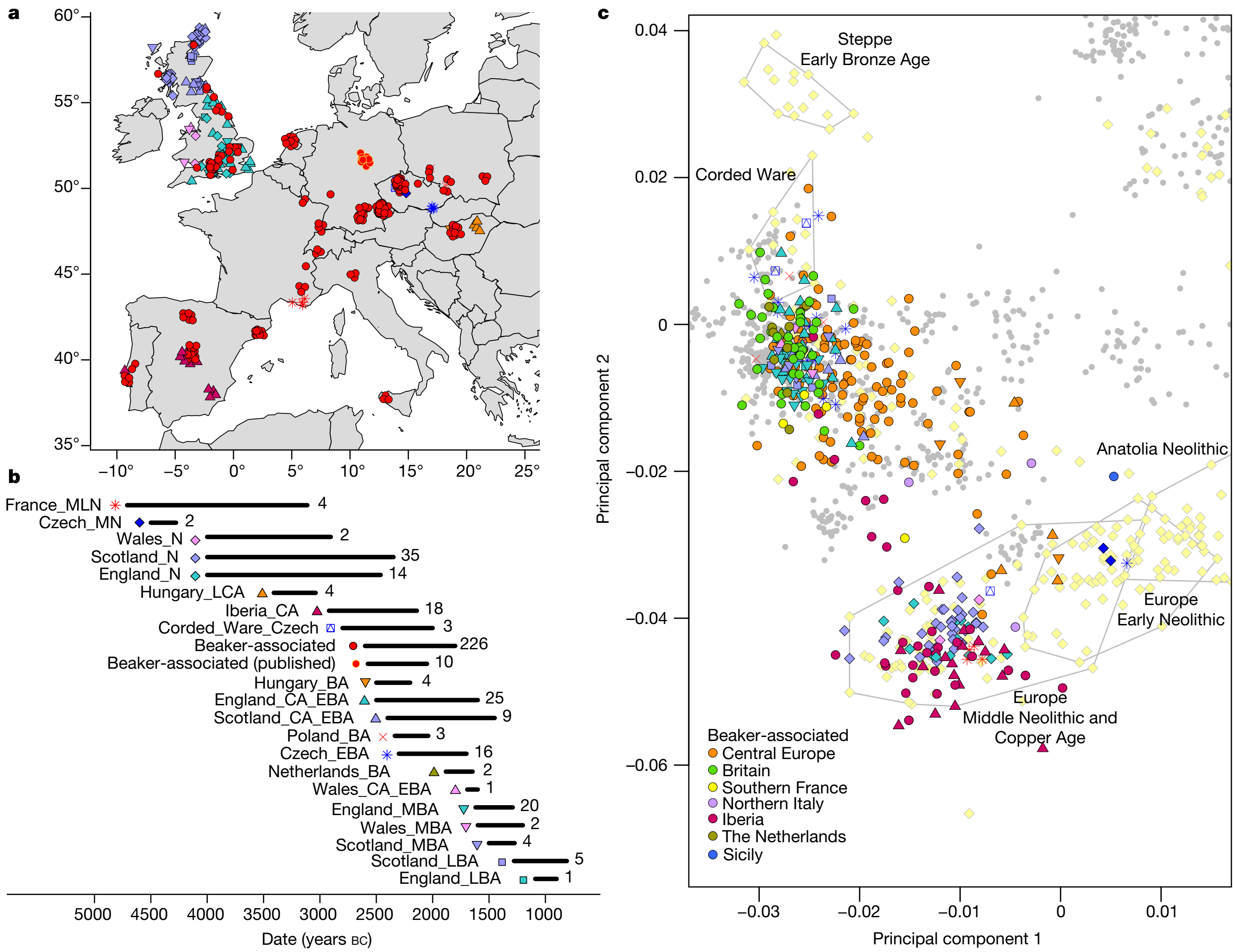

Figure 1 | Spatial, temporal and genetic structure of individuals in this study. a, Geographic distribution of samples with new genome-wide data. Random jitter was added for sites with multiple individuals. Map data from the R package 'maps'. **b**, Approximate time ranges for samples with new genome-wide data. Sample sizes are given next to each bar. **c**, Principal component analysis of 990 present-day west Eurasian individuals (grey dots), with previously published (pale yellow) and new ancient samples projected onto the first two principal components. This figure is a close-up of Extended Data Fig. 3a. See Methods for abbreviations of population names.

as R1b-S116/P312. The widespread presence of the R1b-S116/P312 polymorphism in ancient individuals from central and western Europe suggests that people associated with the Beaker complex may have had an important role in the dissemination of this lineage throughout most of its present-day distribution.

Spread of people associated with the Beaker complex

We performed principal component analysis by projecting the ancient samples onto the genetic variation in a set of west Eurasian present-day populations. We replicated previous findings[11] of two parallel clines, with present-day Europeans on one side and present-day Near Eastern populations on the other (Extended Data Fig. 3a). Individuals associated with the Beaker complex are notably heterogeneous within the European cline along an axis of variation defined by Early Bronze Age Yamnaya individuals from the steppe at one extreme and Middle Neolithic and Copper Age Europeans at the other extreme (Fig. 1c; Extended Data Fig. 3a). This suggests that genetic differentiation among Beaker-complex-associated individuals may be related to variable amounts of steppe-related ancestry. We obtained qualitatively consistent inferences using ADMIXTURE model-based clustering[17]. Beaker-complex-associated individuals harboured three main genetic components: one characteristic of European Mesolithic hunter-gatherers, one maximized in Neolithic individuals from the Levant and Anatolia, and one maximized in Neolithic individuals from Iran and present in admixed form in steppe populations (Extended Data Fig. 3b).

Both principal component analysis and ADMIXTURE are powerful tools for visualizing genetic structure, but they do not provide formal tests of admixture between populations. We grouped Beaker-complex-associated individuals on the basis of geographic proximity and genetic similarity (Supplementary Information section 6), and used qpAdm[2] to directly test admixture models and estimate mixture proportions. We modelled their ancestry as a mixture of Mesolithic western European hunter-gatherers, northwestern Anatolian Neolithic farmers and Early Bronze Age steppe populations; the first two of these contributed to the ancestry of earlier Neolithic Europeans. We find that in areas outside of Iberia, with the exception of Sicily, a large majority of the Beaker-complex-associated individuals that we sampled derive a considerable portion of their ancestry from steppe populations (Fig. 2a). By contrast, in Iberia such ancestry is present in only 8 of the 32 individuals that we analysed; these individuals represent the earliest detection of steppe-related genomic affinities in this region. We observed differences in ancestry not only at a pan-European scale, but also within regions and even within sites. For instance, at Szigetszentmiklós in Hungary, we

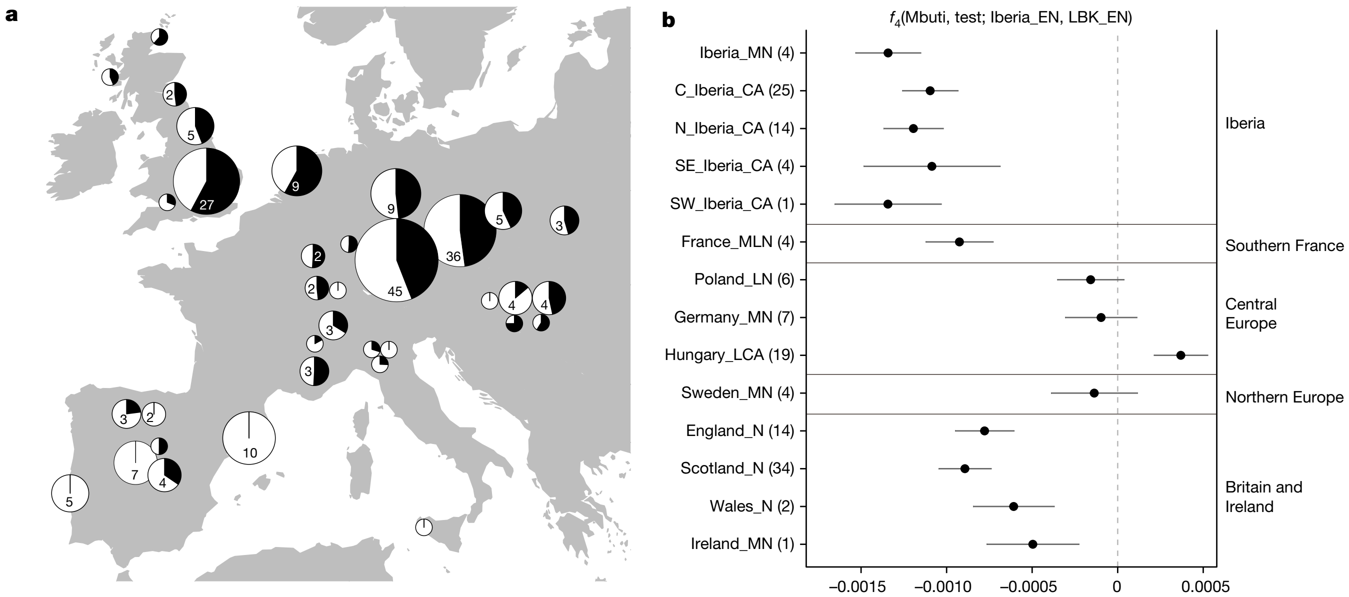

c

		Neolithic/Copper Age source population									
		Iberia_MN	C_Iberia_CA	N_Iberia_CA	SE_Iberia_CA	SW_Iberia_CA	Germany_MN	Poland_LN	Hungary_LCA	Sweden_MN	France_MLN
Test population	Beaker complex Iberia combined	1.66×10^{-1}*	7.23×10^{-1}*	1.76×10^{-5}	1.15×10^{-1}*	6.11×10^{-1}*	8.17×10^{-11}	3.36×10^{-6}	2.72×10^{-59}	6.28×10^{-3}	4.53×10^{-2}
	Beaker complex outside Iberia combined	1.11×10^{-12}	7.48×10^{-10}	2.18×10^{-10}	9.93×10^{-3}	1.04×10^{-2}	2.51×10^{-13}	1.84×10^{-1}*	6.05×10^{-55}	2.45×10^{-1}*	4.61×10^{-4}

Figure 2 | Investigating the genetic makeup of Beaker-complex-associated individuals. a, Proportion of steppe-related ancestry (in black) in Beaker-complex-associated groups computed with qpAdm[2] under the model 'Steppe_EBA + Anatolia_N + WHG' (WHG, Mesolithic western European hunter-gatherers). The area of the pie is proportional to the number of individuals (number shown if more than one). Map data from the R package 'maps'. **b**, *f*-statistics of the form f_4(Mbuti, test; Iberia_EN, LBK_EN) computed for European populations (number of individuals for each group is given in parentheses) before the emergence of the Beaker complex (Supplementary Information section 7). Error bars represent ± 1 standard errors. **c**, Testing different populations as a source for the Neolithic ancestry component in Beaker-complex-associated individuals. The table shows *P* values (* indicates values > 0.05) for the fit of the model: 'Steppe_EBA + Neolithic/Copper Age' source population.

found roughly contemporary Beaker-complex-associated individuals with very different proportions (from 0% to 75%) of steppe-related ancestry. This genetic heterogeneity is consistent with early stages of mixture between previously established European Neolithic populations and migrants with steppe-related ancestry. One implication of this is that even at local scales, the Beaker complex was associated with people of diverse ancestries.

Although the steppe-related ancestry in Beaker-complex-associated individuals had a recent origin in the east[2,3], the other ancestry component—from previously established European populations—could potentially be derived from several parts of Europe, because groups that were genetically closely related were widely distributed during the Neolithic and Copper Ages[2,4,11,16,18–23]. To obtain insight into the origin of this ancestry component in Beaker-complex-associated individuals, we looked for regional patterns of genetic differentiation within Europe during the Neolithic and Copper Age. We examined whether populations pre-dating the emergence of the Beaker complex shared more alleles with Iberian (Iberia_EN) or central European Linearbandkeramik (LBK_EN) Early Neolithic populations (Fig. 2b). As previously described[2], Iberian Middle Neolithic and Copper Age populations, but not central and northern European populations, had genetic affinities with Iberian Early Neolithic farmers (Fig. 2b). These regional patterns could partially be explained by differential genetic affinities to pre-Neolithic hunter-gatherer individuals from different regions[22] (Extended Data Fig. 4). Neolithic individuals from southern France and Britain are also significantly closer to Iberian Early Neolithic farmers than they are to central European Early Neolithic farmers (Fig. 2b), consistent with a previous analysis of a Neolithic genome from Ireland[23]. By modelling Neolithic populations and Mesolithic western European hunter-gatherers in an admixture graph framework, we replicate these results and show that they are not driven by different proportions of hunter-gatherer admixture (Extended Data Fig. 5; Supplementary Information section 7). Our results suggest that a portion of the ancestry of the Neolithic populations of Britain was derived from migrants who spread along the Atlantic coast. Megalithic tombs document substantial interaction along the Atlantic façade of Europe[24], and our results are consistent with such interactions reflecting south-to-north movements of people. More data from southern Britain and Ireland and nearby regions in continental Europe will be needed to fully understand the complex interactions between Britain, Ireland and the continent during the Neolithic[24].

The distinctive genetic signatures found in the Iberian populations who preceded the arrival of Beaker complex, when compared to contemporary central European populations, enable us to formally test for the origin of the Neolithic-related ancestry in Beaker-complex-associated individuals. We grouped individuals from Iberia ($n = 32$) and from outside Iberia ($n = 172$) to increase power and evaluated the fit of different Neolithic and Copper Age groups with qpAdm[2] under the model: 'Steppe_EBA + Neolithic/Copper Age'. For Beaker-complex-associated individuals from Iberia, the best fit was obtained when Middle Neolithic and Copper Age populations from the same region were used as the source for their Neolithic-related ancestry; we could exclude central and northern European populations as sources of this ancestry ($P < 0.0063$) (Fig. 2c). Conversely, the Neolithic-related ancestry in Beaker-complex-associated individuals outside of Iberia was most closely related to central and northern European Neolithic populations with relatively high hunter-gatherer admixture (for example, Poland_LN, $P = 0.18$ and Sweden_MN, $P = 0.25$), and we could significantly exclude Iberian sources ($P < 0.0104$) (Fig. 2c).

These results support mostly different origins for Beaker-complex-associated individuals, with no discernible Iberia-related ancestry outside of Iberia.

Nearly complete turnover of ancestry in Britain

The genetic profile of British Beaker-complex-associated individuals ($n = 37$) shows strong similarities to that of central European Beaker-complex-associated individuals (Extended Data Fig. 3). This observation is not restricted to British individuals associated with the 'All-Over-Cord' Beaker pottery style that is shared between Britain and central Europe: we also find this genetic signal in British individuals associated with Beaker pottery styles derived from the 'Maritime' forms, which were predominant earlier in Iberia. The presence of large amounts of steppe-related ancestry in British Beaker-complex-associated individuals (Fig. 2a) contrasts sharply with Neolithic individuals from Britain ($n = 51$), who have no evidence of steppe genetic affinities and cluster instead with Middle Neolithic and Copper Age populations from mainland Europe (Extended Data Fig. 3). A previous study showed that steppe-related ancestry had arrived in Ireland by the Bronze Age[23]; here we show that, at least in Britain, it arrived earlier in the Copper Age (which, in Britain, is synonymous with the Beaker period).

Among the continental Beaker-complex groups analysed in our dataset, individuals from Oostwoud, the Netherlands, are the most closely related to the large majority of Beaker-complex-associated individuals from southern Britain ($n = 27$). The two groups had almost identical steppe-related ancestry proportions (Fig. 2a), the highest level of shared genetic drift (Extended Data Fig. 6b) and were symmetrically related to most ancient populations (Extended Data Fig. 6a), which shows that they are likely derived from the same ancestral population with limited mixture into either group. This does not necessarily imply that the Oostwoud individuals are direct ancestors of the British individuals, but it does show that they were closely related genetically to the population—perhaps yet to be sampled—that moved into Britain from continental Europe.

We investigated the magnitude of population replacement in Britain with qpAdm[2] by modelling the genome-wide ancestry of Neolithic, Copper and Bronze Age individuals, including Beaker-complex-associated individuals, as a mixture of continental Beaker-complex-associated samples (using the Oostwoud individuals as a surrogate) and the British Neolithic population (Supplementary Information section 8). During the first centuries after the initial contact, between approximately 2450 and 2000 BC, ancestry proportions were variable (Fig. 3), which is consistent with migrant communities just beginning to mix with the previously established British Neolithic population. After roughly 2000 BC, individuals were more homogeneous and possessed less variation in ancestry proportions and a modest increase in Neolithic-related ancestry (Fig. 3). This could represent admixture with persisting British populations with high levels of Neolithic-related ancestry or, alternatively, with incoming continental populations with higher proportions of Neolithic-related ancestry. In either case, our results imply a minimum of $90 \pm 2\%$ local population turnover by the Middle Bronze Age (approximately 1500–1000 BC), with no significant decrease observed in 5 samples from the Late Bronze Age. Although the exact turnover rate and its geographic pattern await refinement with more ancient samples, our results imply that for individuals from Britain during and after the Beaker period, a very high fraction of their DNA derives from ancestors who lived in continental Europe before 2450 BC. An independent line of evidence for population turnover comes from uniparental markers. Whereas Y-chromosome haplogroup R1b was completely absent in Neolithic individuals ($n = 33$), it represents more than 90% of the Y chromosomes in individuals from Copper and Bronze Age Britain ($n = 52$) (Fig. 3). The introduction of new mtDNA haplogroups, such as I, R1a and U4, which were present in Beaker-complex-associated populations from continental Europe but not in Neolithic Britain (Supplementary Table 3), suggests that both men and women were involved in this population turnover.

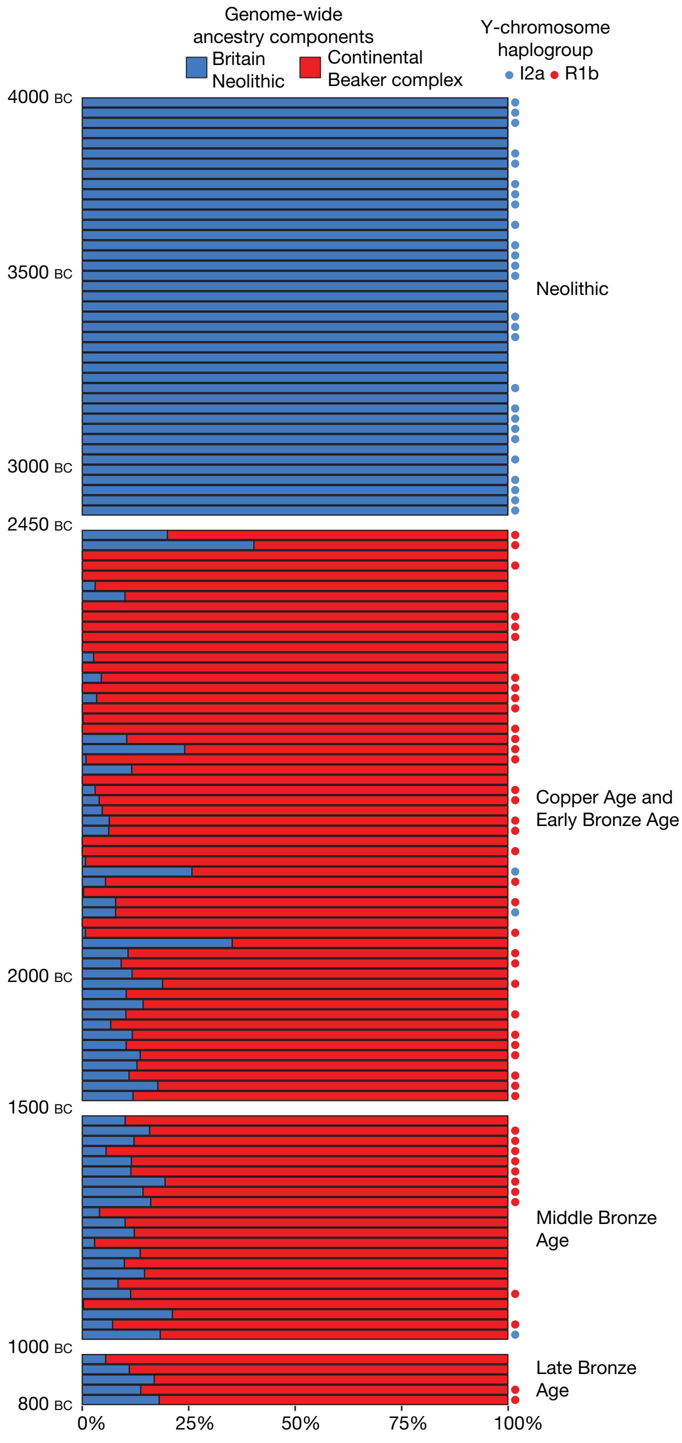

Figure 3 | Population transformation in Britain associated with the arrival of the Beaker complex. Modelling Neolithic, Copper and Bronze Age (including Beaker-complex-associated) individuals from Britain as a mixture of continental Beaker-complex-associated individuals (red) and the Neolithic population from Britain (blue). Each bar represents genome-wide mixture proportions for one individual. Individuals are ordered chronologically and included in the plot if represented by more than 100,000 SNPs. Circles indicate the Y-chromosome haplogroup for male individuals.

Our ancient DNA transect-through-time in Britain also enabled us to track the frequencies of alleles with known phenotypic effects. Derived alleles at rs16891982 in *SLC45A2* and rs12913832 in *HERC2/OCA2*, which contribute to reduced skin and eye pigmentation in Europeans, considerably increased in frequency between the Neolithic period and the Beaker and Bronze Age periods (Extended Data Fig. 7). The arrival of migrants associated with the Beaker complex therefore markedly altered the pigmentation phenotypes of British populations. However, the lactase persistence allele at SNP rs4988235 in *LCT* remained at very low frequencies across this transition, both in Britain and continental Europe, which shows that the major increase in its frequency occurred within the last 3,500 years[3,4,25].

Discussion

The term 'Bell Beaker' was introduced by late-nineteenth- and early-twentieth-century archaeologists to refer to a distinctive pottery style found across western and central Europe at the end of the Neolithic that was initially hypothesized to have been spread by a genetically homogeneous population. This idea of a 'Beaker Folk' became unpopular after the 1960s as scepticism grew about the role of migration in mediating change in archaeological cultures[26], although even at the time[27] it was speculated that the expansion of the Beaker complex into Britain was an exception—a prediction that has now been borne out by ancient genomic data.

The expansion of the Beaker complex cannot be described by a simple one-to-one mapping of an archaeologically defined material culture to a genetically homogeneous population. This stands in contrast to other archaeological complexes, notably the Linearbandkeramik farmers of central Europe[2], the Early Bronze Age Yamnaya of the steppe[2,3] and—to some extent—the Corded Ware complex of central and eastern Europe[2,3]. Our results support a model in which cultural transmission and human migration both had important roles, with the relative balance of these two processes depending on the region. In Iberia, the majority of Beaker-complex-associated individuals lacked steppe affinities and were genetically most similar to preceding Iberian populations. In central Europe, steppe-related ancestry was widespread and we can exclude a substantial contribution from Iberian Beaker-complex-associated individuals. However, the presence of steppe-related ancestry in some Iberian individuals demonstrates that gene flow into Iberia was not uncommon during this period. These results contradict initial suggestions of gene flow into central Europe based on analysis of mtDNA[28] and dental morphology[29]. In particular, mtDNA haplogroups H1 and H3 were proposed as markers for a Beaker-complex expansion originating in Iberia[28], yet H3 is absent among our Iberian Beaker-complex-associated individuals.

In other parts of Europe, the expansion of the Beaker complex was driven to a substantial extent by migration. This genomic transformation is clearest in Britain owing to our densely sampled time transect. The arrival of people associated with the Beaker complex precipitated a demographic transformation in Britain, exemplified by the presence of individuals with large amounts of steppe-related ancestry after 2450 BC. We considered the possibility that an uneven geographic distribution of samples may have caused us to miss a major population that lacked steppe-derived ancestry after 2450 BC. However, our British Beaker and Bronze Age samples are dispersed geographically—extending from the southeastern peninsula of England to the Western Isles of Scotland—and come from a wide variety of funerary contexts (rivers, caves, pits, barrows, cists and flat graves) and diverse funerary traditions (single and multiple burials in variable states of anatomical articulation), which reduces the likelihood that our sampling missed major populations. We also considered the possibility that different burial practices between local and incoming populations (cremation versus inhumation) during the early stages of interaction could result in a sampling bias against local individuals. Although it is possible that such a sampling bias makes the ancestry transition appear more sudden than it in fact was, the long-term demographic effect was clearly substantial, as the pervasive steppe-related ancestry observed during the Beaker period, which was absent in the Neolithic period, persisted during the Bronze Age—and indeed remains predominant in Britain today[2]. These results are notable in light of strontium and oxygen isotope analyses of British skeletons from the Beaker and Bronze Age periods[30], which have provided no evidence for substantial mobility over individuals' lifetimes from locations with cooler climates or from places with geologies atypical of Britain. However, the isotope data are only sensitive to first-generation migrants and do not rule out movements from regions such as the lower Rhine area or from other geologically similar regions for which DNA sampling is still sparse. Further sampling of regions on the European continent may reveal additional candidate sources.

By analysing DNA data from ancient individuals, we have been able to provide constraints on the interpretations of the processes underlying cultural and social changes in Europe during the third millennium BC. Our results motivate further archaeological research to identify the changes in social organization, technology, subsistence, climate, population sizes[31] or pathogen exposure[32,33] that could have precipitated the demographic changes uncovered in this study.

Online Content Methods, along with any additional Extended Data display items and Source Data, are available in the online version of the paper; references unique to these sections appear only in the online paper.

Received 8 May 2017; accepted 4 January 2018.
Published online 21 February 2018.

1. Czebreszuk, J. In *Ancient Europe, 8000 B.C. to A.D. 1000: An Encyclopedia of the Barbarian World* (eds Bogucki, P. I. & Crabtree, P. J.) 476–485 (Charles Scribner's Sons, 2004).
2. Haak, W. *et al.* Massive migration from the steppe was a source for Indo-European languages in Europe. *Nature* **522,** 207–211 (2015).
3. Allentoft, M. E. *et al.* Population genomics of Bronze Age Eurasia. *Nature* **522,** 167–172 (2015).
4. Mathieson, I. *et al.* Genome-wide patterns of selection in 230 ancient Eurasians. *Nature* **528,** 499–503 (2015).
5. Czebreszuk, J. *Similar But Different. Bell Beakers in Europe* (Adam Mickiewicz Univ., 2004).
6. Cardoso, J. L. Absolute chronology of the Beaker phenomenon north of the Tagus estuary: demographic and social implications. *Trab. Prehist.* **71,** 56–75 (2014).
7. Jeunesse, C. The dogma of the Iberian origin of the Bell Beaker: attempting its deconstruction. *J. Neolit. Archaeol.* **16,** 158–166 (2015).
8. Fokkens, H. & Nicolis, F. *Background to Beakers. Inquiries into Regional Cultural Backgrounds of the Bell Beaker Complex* (Sidestone, 2012).
9. Linden, M. V. What linked the Bell Beakers in third millennium BC Europe? *Antiquity* **81,** 343–352 (2007).
10. Fu, Q. *et al.* An early modern human from Romania with a recent Neanderthal ancestor. *Nature* **524,** 216–219 (2015).
11. Lazaridis, I. *et al.* Ancient human genomes suggest three ancestral populations for present-day Europeans. *Nature* **513,** 409–413 (2014).
12. Lazaridis, I. *et al.* Genomic insights into the origin of farming in the ancient Near East. *Nature* **536,** 419–424 (2016).
13. Mallick, S. *et al.* The Simons Genome Diversity Project: 300 genomes from 142 diverse populations. *Nature* **538,** 201–206 (2016).
14. Valverde, L. *et al.* New clues to the evolutionary history of the main European paternal lineage M269: dissection of the Y-SNP S116 in Atlantic Europe and Iberia. *Eur. J. Hum. Genet.* **24,** 437–441 (2016).
15. Gamba, C. *et al.* Ancient DNA from an Early Neolithic Iberian population supports a pioneer colonization by first farmers. *Mol. Ecol.* **21,** 45–56 (2012).
16. Günther, T. *et al.* Ancient genomes link early farmers from Atapuerca in Spain to modern-day Basques. *Proc. Natl Acad. Sci. USA* **112,** 11917–11922 (2015).
17. Alexander, D. H., Novembre, J. & Lange, K. Fast model-based estimation of ancestry in unrelated individuals. *Genome Res.* **19,** 1655–1664 (2009).
18. Broushaki, F. *et al.* Early Neolithic genomes from the eastern Fertile Crescent. *Science* **353,** 499–503 (2016).
19. Skoglund, P. *et al.* Genomic diversity and admixture differs for Stone-Age Scandinavian foragers and farmers. *Science* **344,** 747–750 (2014).
20. Olalde, I. *et al.* A common genetic origin for early farmers from Mediterranean Cardial and central European LBK cultures. *Mol. Biol. Evol.* **32,** 3132–3142 (2015).
21. Mathieson, I. *et al.* The genomic history of southeastern Europe. *Nature* https://doi.org/10.1038/nature25778 (2018).
22. Lipson, M. *et al.* Parallel palaeogenomic transects reveal complex genetic history of early European farmers. *Nature* **551,** 368–372 (2017).
23. Cassidy, L. M. *et al.* Neolithic and Bronze Age migration to Ireland and establishment of the insular Atlantic genome. *Proc. Natl Acad. Sci. USA* **113,** 368–373 (2016).
24. Sheridan, J. A. In *Landscapes in Transition* (eds Finlayson, B. & Warren, G.) 89–105 (Oxbow, 2010).

25. Burger, J., Kirchner, M., Bramanti, B., Haak, W. & Thomas, M. G. Absence of the lactase-persistence-associated allele in early Neolithic Europeans. *Proc. Natl Acad. Sci. USA* **104,** 3736–3741 (2007).
26. Clarke, D. L. In *Glockenbecher Symposion, Oberried, 18–23 März 1974* (eds Lanting, J. N. & van DerWaals, J. D.) 460–477 (Bussum, 1976).
27. Clark, G. The invasion hypothesis in British archaeology. *Antiquity* **40,** 172–189 (1966).
28. Brotherton, P. *et al.* Neolithic mitochondrial haplogroup H genomes and the genetic origins of Europeans. *Nat. Commun.* **4,** 1764 (2013).
29. Desideri, J. *When Beakers Met Bell Beakers: an Analysis of Dental Remains (British Archaeological Reports International Series 2292)* (Archaeopress, 2011).
30. Parker Pearson, M. *et al.* Beaker people in Britain: migration, mobility and diet. *Antiquity* **90,** 620–637 (2016).
31. Shennan, S. *et al.* Regional population collapse followed initial agriculture booms in mid-Holocene Europe. *Nat. Commun.* **4,** 2486 (2013).
32. Valtueña, A. A. *et al.* The Stone Age plague and its persistence in Eurasia. *Curr. Biol.* **27,** 3683–3691 (2017).
33. Rasmussen, S. *et al.* Early divergent strains of *Yersinia pestis* in Eurasia 5,000 years ago. *Cell* **163,** 571–582 (2015).

Supplementary Information is available in the online version of the paper.

Acknowledgements We thank D. Anthony, J. Koch, I. Mathieson and C. Renfrew for comments; A. Cooper for support from the Australian Centre for Ancient DNA; the Bristol Radiocarbon Accelerator Mass Spectrometry Facility (BRAMS); A. C. Sousa, A. M. Cólliga, L. Loe, C. Roth, E. Carmona Ballesteros, M. Kunst, S.-A. Coupar, M. Giesen, T. Lord, M. Green, A. Chamberlain and G. Drinkall for assistance with samples; E. Willerslev for supporting several co-authors at the Centre for GeoGenetics; the Museo Arqueológico Regional de la Comunidad de Madrid, the Hunterian Museum, University of Glasgow, the Orkney Museum, the Museu Municipal de Torres Vedras, the Great North Museum: Hancock, the Society of Antiquaries of Newcastle upon Tyne, the Sunderland Museum, the National Museum of Wales, the Duckworth Laboratory, the Wiltshire Museum, the Wells Museum, the Brighton Museum, the Somerset Heritage Museum and the Museum of London for facilitating sample collection. Support for this project was provided by Czech Academy of Sciences grant RVO:67985912; by the Momentum Mobility Research Group of the Hungarian Academy of Sciences; by the Wellcome Trust (100713/Z/12/Z); by Irish Research Council grant GOIPG/2013/36 to D.F.; by the Heidelberg Academy of Sciences (WIN project 'Times of Upheaval') to P.W.S., J.K. and A.Mi.; by the Swedish Foundation for Humanities and Social Sciences grant M16-0455:1 to K.Kr.; by the National Science Centre, Poland grant DEC-2013/10/E/HS3/00141 to M.Fu.; by a Spanish MINECO grant BFU2015-64699-P to C.L.-F.; by Obra Social La Caixa and a Spanish MINECO grant HAR2016-77600-P to C.L., P.R. and C.Bl.; by the NSF Archaeometry program BCS-1460369 to D.J.K.; by the NFS Archaeology program BCS-1725067 to D.J.K. and T.Ha.; and by an Allen Discovery Center grant from the Paul Allen Foundation, US National Science Foundation HOMINID grant BCS-1032255, US National Institutes of Health grant GM100233, and the Howard Hughes Medical Institute to D.R.

Author Contributions S.B., M.E.A., N.R., A.S.-N., A.Mi., N.B., M.Fe., E.Har., M.Mi., J.O., K.S., O.C., D.K., F.C., R.Pi., J.K., W.H., I.B. and D.R. performed or supervised laboratory work. G.T.C. and D.J.K. undertook the radiocarbon dating of a large fraction of samples. I.A., K.Kr., A.B., K.W.A., A.A.F., E.B., M.B.-B., D.B., C.Bl., J.V.M., R.M.G., C.Bo., L.Bo., T.A., L.Bü., S.C., L.C.N., O.E.C., G.T.C., B.C., A.D., K.E.D., N.D., M.E., C.E., M.K., J.F.F., H.F., C.F., M.G., R.G.P., M.H.-U., E.Had., G.H., N.J., T.K., K.Ma., S.P., P.L., O.L., A.L., C.H.M., V.G.O., A.B.R., J.L.M., T.M., J.I.M., K.Mc., B.G.M., A.Mo., G.K., V.K., A.C., R.Pa., A.E., K.Kö., T.Ha., T.S., J.Da., Z.B., M.H., P.V., M.D., F.B., R.F.F., A.-M.H.-C., S.T., E.C., L.L., A.V., A.Z., C.W., G.D., E.G.-D., B.N., M.Br., M.Lu., R.M., J.De., M.Be., G.B., M.Fu., A.H., M.Ma., A.R., S.L., I.S., K.T.L., J.L.C., C.L., M.P.P., P.W., T.D.P., P.P., P.-J.R., P.R., R.R., M.A.R.G., A.Sc., J.S., A.M.S., V.S., L.V., J.Z., D.C., T.Hi., V.H., A.Sh., K.-G.S., P.W.S., R.Pi., J.K., W.H., I.B., C.L.-F. and D.R. assembled archaeological material. I.O., S.M., T.B., A.Mi., E.A., M.Li., I.L., N.P., Y.D., Z.F., D.F., D.J.K., P.d.K., T.K.H., M.G.T. and D.R. analysed data. I.O., C.L.-F. and D.R. wrote the manuscript with input from all co-authors.

Author Information Reprints and permissions information is available at www.nature.com/reprints. The authors declare no competing financial interests. Readers are welcome to comment on the online version of the paper. Publisher's note: Springer Nature remains neutral with regard to jurisdictional claims in published maps and institutional affiliations. Correspondence and requests for materials should be addressed to I.O. (inigo_olalde@hms.harvard.edu) or D.R. (reich@genetics.med.harvard.edu).

Reviewer Information *Nature* thanks C. Renfrew, E. Rhodes, M. Richards and the other anonymous reviewer(s) for their contribution to the peer review of this work.

Iñigo Olalde[1], Selina Brace[2], Morten E. Allentoft[3], Ian Armit[4]§, Kristian Kristiansen[5]§, Thomas Booth[2], Nadin Rohland[1], Swapan Mallick[1,6,7], Anna Szécsényi-Nagy[8], Alissa Mittnik[9,10], Eveline Altena[11], Mark Lipson[1], Iosif Lazaridis[1,6], Thomas K. Harper[12], Nick Patterson[6], Nasreen Broomandkhoshbacht[1,7], Yoan Diekmann[13], Zuzana Faltyskova[13], Daniel Fernandes[14,15,16], Matthew Ferry[1,7], Eadaoin Harney[1], Peter de Knijff[11], Megan Michel[1,7], Jonas Oppenheimer[1,7], Kristin Stewardson[1,7], Alistair Barclay[17], Kurt Werner Alt[18,19,20], Corina Liesau[21], Patricia Ríos[21], Concepción Blasco[21], Jorge Vega Miguel[22], Roberto Menduiña García[22], Azucena Avilés Fernández[23], Eszter Bánffy[24,25], Maria Bernabò-Brea[26], David Billoin[27], Clive Bonsall[28], Laura Bonsall[29], Tim Allen[30], Lindsey Büster[4], Sophie Carver[31], Laura Castells Navarro[4], Oliver E. Craig[32], Gordon T. Cook[33], Barry Cunliffe[34], Anthony Denaire[35], Kirsten Egging Dinwiddy[17], Natasha Dodwell[36], Michal Ernée[37], Christopher Evans[38], Milan Kuchařík[39], Joan Francès Farré[40], Chris Fowler[41], Michiel Gazenbeek[42], Rafael Garrido Pena[21], María Haber-Uriarte[23], Elżbieta Haduch[43], Gill Hey[30], Nick Jowett[44], Timothy Knowles[45], Ken Massy[46], Saskia Pfrengle[9], Philippe Lefranc[47], Olivier Lemercier[48], Arnaud Lefebvre[49,50], César Heras Martínez[51,52,53], Virginia Galera Olmo[52,53], Ana Bastida Ramírez[51], Joaquín Lomba Maurandi[23], Tona Majó[54], Jacqueline I. McKinley[17], Kathleen McSweeney[28], Balázs Gusztáv Mende[8], Alessandra Mod[55], Gabriella Kulcsár[24], Viktória Kiss[24], András Czene[56], Róbert Patay[57], Anna Endrődi[58], Kitti Köhler[24], Tamás Hajdu[59,60], Tamás Szeniczey[59], János Dani[61], Zsolt Bernert[60], Maya Hoole[62], Olivia Cheronet[14,15], Denise Keating[63], Petr Velemínský[64], Miroslav Dobeš[37], Francesca Candilio[65,66,67], Fraser Brown[30], Raúl Flores Fernández[68], Ana-Mercedes Herrero-Corral[69], Sebastiano Tusa[70], Emiliano Carnieri[71], Luigi Lentini[72], Antonella Valenti[73], Alessandro Zanini[74], Clive Waddington[75], Germán Delibes[76], Elisa Guerra-Doce[76], Benjamin Neil[38], Marcus Brittain[38], Mike Luke[77], Richard Mortimer[36], Jocelyne Desideri[78], Marie Besse[78], Günter Brücken[79], Mirosław Furmanek[80], Agata Hałuszko[80], Maksym Mackiewicz[80], Artur Rapiński[81], Stephany Leach[82], Ignacio Soriano[83], Katina T. Lillios[84], João Luís Cardoso[85,86], Michael Parker Pearson[87], Piotr Włodarczak[88], T. Douglas Price[89], Pilar Prieto[90], Pierre-Jérôme Rey[91], Roberto Risch[83], Manuel A. Rojo Guerra[92], Aurore Schmitt[93], Joël Serralongue[94], Ana Maria Silva[95], Václav Smrčka[96], Luc Vergnaud[97], João Zilhão[85,98,99], David Caramelli[55], Thomas Higham[100], Mark G. Thomas[13], Douglas J. Kennett[101], Harry Fokkens[102], Volker Heyd[31,103], Alison Sheridan[104], Karl-Göran Sjögren[5], Philipp W. Stockhammer[46,105], Johannes Krause[105], Ron Pinhasi[14,15]§, Wolfgang Haak[105,106]§, Ian Barnes[2]§, Carles Lalueza-Fox[107]§ & David Reich[1,6,7]§

[1]Department of Genetics, Harvard Medical School, Boston, Massachusetts 02115, USA. [2]Department of Earth Sciences, Natural History Museum, London SW7 5BD, UK. [3]Centre for GeoGenetics, Natural History Museum, University of Copenhagen, Copenhagen 1350, Denmark. [4]School of Archaeological and Forensic Sciences, University of Bradford, Bradford BD7 1DP, UK. [5]University of Gothenburg, Gothenburg 405 30, Sweden. [6]Broad Institute of MIT and Harvard, Cambridge, Massachusetts 02142, USA. [7]Howard Hughes Medical Institute, Harvard Medical School, Boston, Massachusetts 02115, USA. [8]Laboratory of Archaeogenetics, Institute of Archaeology, Research Centre for the Humanities, Hungarian Academy of Sciences, Budapest 1097, Hungary. [9]Institute for Archaeological Sciences, Archaeo- and Palaeogenetics, University of Tübingen, Tübingen 72070, Germany. [10]Department of Archaeogenetics, Max Planck Institute for the Science of Human History, Jena 07745, Germany. [11]Department of Human Genetics, Leiden University Medical Center, Leiden 2333 ZC, The Netherlands. [12]Department of Anthropology, The Pennsylvania State University, University Park, Pennsylvania 16802, USA. [13]Research Department of Genetics, Evolution and Environment, University College London, London WC1E 6BT, UK. [14]Earth Institute and School of Archaeology, University College Dublin, Dublin 4, Ireland. [15]Department of Anthropology, University of Vienna, Vienna 1090, Austria. [16]Research Center for Anthropology and Health, Department of Life Science, University of Coimbra, Coimbra 3000-456, Portugal. [17]Wessex Archaeology, Salisbury SP4 6EB, UK. [18]Center of Natural and Cultural History of Man, Danube Private University, Krems 3500, Austria. [19]Department of Biomedical Engineering, Basel University, Basel 4123, Switzerland. [20]Integrative Prehistory and Archaeological Science, Basel University, Basel, Switzerland. [21]Departamento de Prehistoria y Arqueología, Universidad Autónoma de Madrid, Madrid 28049, Spain. [22]ARGEA S.L., Madrid 28011, Spain. [23]Área de Prehistoria, Universidad de Murcia, Murcia 30001, Spain. [24]Institute of Archaeology, Research Centre for the Humanities, Hungarian Academy of Sciences, Budapest 1097, Hungary. [25]Romano-Germanic Commission, German Archaeological Institute, Frankfurt am Main 60325, Germany. [26]Museo Archeologico Nazionale di Parma, Parma 43100, Italy. [27]INRAP, Institut National de Recherches Archéologiques Préventives, Buffard 25440, France. [28]School of History, Classics and Archaeology, University of Edinburgh, Edinburgh EH8 9AG, UK. [29]10 Merchiston Gardens, Edinburgh EH10 5DD, UK. [30]Oxford Archaeology, Oxford OX2 0ES, UK. [31]Department of Archaeology and Anthropology, University of Bristol, Bristol BS8 1UU, UK. [32]BioArCh, Department of Archaeology, University of York, York YO10 5DD, UK. [33]Scottish Universities Environmental Research Centre, East Kilbride G75 0QF, UK. [34]Institute of Archaeology, University of Oxford, Oxford OX1 2PG, UK. [35]University of Burgundy, Dijon 21000, France. [36]Oxford Archaeology East, Cambridge CB23 8SQ, UK. [37]Institute of Archaeology, Czech Academy of Sciences, Prague 118 01, Czech Republic. [38]Cambridge Archaeological Unit, Department of Archaeology, University of Cambridge, Cambridge CB3 0DT, UK. [39]Labrys o.p.s., Prague 198 00, Czech Republic. [40]Museu i Poblat Ibèric de Ca n'Oliver, Cerdanyola del Vallès 08290, Spain. [41]School of History, Classics & Archaeology, Newcastle University, Newcastle upon Tyne NE1 7RU, UK. [42]INRAP, Institut National de Recherches Archéologiques Préventives, Nice 06300, France. [43]Institute of Zoology and Biomedical Research, Jagiellonian University, Kraków 31-007, Poland. [44]Great Orme Mines, Great Orme, Llandudno LL30 2XG, UK. [45]Bristol Radiocarbon Accelerator Mass Spectrometry Facility, University of Bristol, Bristol BS8 1UU, UK. [46]Institut für Vor- und Frühgeschichtliche Archäologie und Provinzialrömische Archäologie,

Ludwig-Maximilians-Universität München, Munich 80539, Germany. [47]INRAP, Institut National de Recherches Archéologiques Préventives, Strasbourg 67100, France. [48]Université Paul-Valéry - Montpellier 3, UMR 5140 ASM, Montpellier 34199, France. [49]INRAP, Institut National de Recherches Archéologiques Préventives, Metz 57063, France. [50]UMR 5199, Pacea, équipe A3P, Université de Bordeaux, Talence 33400, France. [51]TRÉBEDE, Patrimonio y Cultura SL, Torres de la Alameda 28813, Spain. [52]Departamento de Ciencias de la Vida, Universidad de Alcalá, Alcalá de Henares 28801, Spain. [53]Instituto Universitario de Investigación en Ciencias Policiales (IUICP), Alcalá de Henares 28801, Spain. [54]Archaeom, Departament de Prehistòria, Universitat Autònoma de Barcelona, Cerdanyola del Vallès 08193, Spain. [55]Department of Biology, University of Florence, Florence 50121, Italy. [56]Salisbury Ltd, Budaörs 2040, Hungary. [57]Ferenczy Museum Center, Szentendre 2100, Hungary. [58]Budapest History Museum, Budapest 1014, Hungary. [59]Department of Biological Anthropology, Eötvös Loránd University, Budapest 1117, Hungary. [60]Hungarian Natural History Museum, Budapest 1083, Hungary. [61]Déri Museum, Debrecen 4026, Hungary. [62]Historic Environment Scotland, Edinburgh EH9 1SH, UK. [63]Humanities Institute, University College Dublin, Dublin 4, Ireland. [64]Department of Anthropology, National Museum, Prague 115 79, Czech Republic. [65]Soprintendenza Archeologia belle arti e paesaggio per la città metropolitana di Cagliari e per le province di Oristano e Sud Sardegna, Cagliari 9124, Italy. [66]Physical Anthropology Section, University of Philadelphia Museum of Archaeology and Anthropology, Philadelphia, Pennsylvania 19104, USA. [67]Department of Environmental Biology, Sapienza University of Rome, Rome 00185, Italy. [68]46 Cuidad Real Street, Parla 28982, Spain. [69]Departamento de Prehistoria, Universidad Complutense de Madrid, Madrid 28040, Spain. [70]Soprintendenza del Mare, Palermo 90133, Italy. [71]Facoltà di Lettere e Filosofia, Università di Palermo, Palermo 90133, Italy. [72]Soprintendenza per i beni culturali e ambientali di Trapani, Trapani 91100, Italy. [73]Prima Archeologia del Mediterraneo, Partanna 91028, Italy. [74]Università degli Studi di Palermo, Agrigento 92100, Italy. [75]Archaeological Research Services Ltd, Bakewell DE45 1HB, UK. [76]Departamento de Prehistoria, Facultad de Filosofía y Letras, Universidad de Valladolid, Valladolid 47011, Spain. [77]Albion Archaeology, Bedford MK42 0AS, UK. [78]Laboratory of Prehistoric Archaeology and Anthropology, Department F.-A. Forel for Environmental and Aquatic Sciences, University of Geneva, Geneva 4, Switzerland. [79]General Department of Cultural Heritage Rhineland Palatinate, Department of Archaeology, Mainz 55116, Germany. [80]Institute of Archaeology, University of Wroclaw, Wrocław 50-137, Poland. [81]Institute of Archaeology, Silesian University in Opava, Opava 746 01, Czech Republic. [82]Department of Archaeology, University of Exeter, Exeter EX4 4QE, UK. [83]Departament de Prehistòria, Universitat Autònoma de Barcelona, Cerdanyola del Vallès 08193, Spain. [84]Department of Anthropology, University of Iowa, Iowa City, Iowa 52240, USA. [85]Centro de Arqueologia, Universidade de Lisboa, Lisboa 1600-214, Portugal. [86]Universidade Aberta, Lisboa 1269-001, Portugal. [87]Institute of Archaeology, University College London, London WC1H 0PY, UK. [88]Institute of Archaeology and Ethnology, Polish Academy of Sciences, Kraków 31-016, Poland. [89]Laboratory for Archaeological Chemistry, University of Wisconsin-Madison, Madison, Wisconsin 53706, USA. [90]University of Santiago de Compostela, Santiago de Compostela 15782, Spain. [91]UMR 5204 Laboratoire Edytem, Université Savoie Mont Blanc, Chambéry 73376, France. [92]Department of Prehistory and Archaeology, Faculty of Philosophy and Letters, Valladolid University, Valladolid 47011, Spain. [93]UMR 7268 ADES, CNRS, Aix-Marseille Univ, EFS, Faculté de médecine Nord, Marseille 13015, France. [94]Service archéologique, Conseil Général de la Haute-Savoie, Annecy 74000, France. [95]Laboratory of Prehistory, Research Center for Anthropology and Health, Department of Life Science, University of Coimbra, Coimbra 3000-456, Portugal. [96]Institute for History of Medicine and Foreign Languages, First Faculty of Medicine, Charles University, Prague 121 08, Czech Republic. [97]ANTEA Bureau d'étude en Archéologie, Habsheim 68440, France. [98]Institució Catalana de Recerca i Estudis Avançats, Barcelona 08010, Spain. [99]Departament d'Història i Arqueologia, Universitat de Barcelona, Barcelona 08001, Spain. [100]Oxford Radiocarbon Accelerator Unit, RLAHA, University of Oxford, Oxford OX1 3QY, UK. [101]Department of Anthropology & Institute for Energy and the Environment, The Pennsylvania State University, University Park, Pennsylvania 16802, USA. [102]Faculty of Archaeology, Leiden University, 2333 CC Leiden, The Netherlands. [103]Department of Philosophy, History, Culture and Art Studies, Section of Archaeology, University of Helsinki, Helsinki 00014, Finland. [104]National Museums Scotland, Edinburgh EH1 1JF, UK. [105]Max Planck Institute for the Science of Human History, Jena 07745, Germany. [106]Australian Centre for Ancient DNA, School of Biological Sciences, University of Adelaide, Adelaide 5005, South Australia, Australia. [107]Institute of Evolutionary Biology, CSIC-Universitat Pompeu Fabra, Barcelona 08003, Spain.
§These authors jointly supervised this work.

METHODS

No statistical methods were used to predetermine sample size. The experiments were not randomized and the investigators were not blinded to allocation during experiments and outcome assessment.

Ancient DNA analysis. We screened skeletal samples for DNA preservation in dedicated clean rooms. We extracted DNA[34–36] and prepared barcoded next-generation sequencing libraries, the majority of which were treated with uracil-DNA glycosylase (UDG) to greatly reduce the damage (except at the terminal nucleotide) that is characteristic of ancient DNA[37,38] (Supplementary Information section 4). We initially enriched libraries for sequences overlapping the mitochondrial genome[39] and approximately 3,000 nuclear SNPs, using synthesized baits (CustomArray) that we PCR-amplified. We sequenced the enriched material on an Illumina NextSeq instrument with 2×76 cycles, and 2×7 cycles to read out the two indices[40]. We merged read pairs with the expected barcodes that overlapped by at least 15 bases, mapped the merged sequences to the human reference genome hg19 and to the reconstructed mitochondrial DNA consensus sequence[41] using the 'samse' command in bwa v.0.6.1[42], and then removed duplicated sequences. We evaluated DNA authenticity by estimating the rate of mismatching to the consensus mitochondrial sequence[43], and also by requiring that the rate of damage at the terminal nucleotide was at least 3% for UDG-treated libraries[43] and 10% for non-UDG-treated libraries[44].

For libraries that appeared promising after screening, we enriched in two consecutive rounds for sequences overlapping 1,233,013 SNPs ('1,240k SNP capture')[2,10] and sequenced 2×76 cycles and 2×7 cycles on an Illumina NextSeq500 instrument. We bioinformatically processed the data in the same way as for the mitochondrial capture data, except that this time we mapped only to hg19 and merged the data from different libraries of the same individual. We further evaluated authenticity by looking at the ratio of X-to-Y chromosome reads and estimating X-chromosome contamination in males based on the rate of heterozygosity[45]. Samples with evidence of contamination were either filtered out or restricted to sequences with terminal cytosine deamination in order to remove sequences that derived from modern contaminants. Finally, we filtered out samples with fewer than 10,000 targeted SNPs covered at least once and samples that were first-degree relatives of others in the dataset (keeping the sample with the larger number of covered SNPs) (Supplementary Table 1) from our genome-wide analysis dataset.

Mitochondrial haplogroup determination. We used the mitochondrial capture .bam files to determine the mitochondrial haplogroup of each sample with new data, restricting our analysis to sequences with MAPQ ≥ 30 and base quality ≥ 30. First, we constructed a consensus sequence with samtools and bcftools[46], using a majority rule and requiring a minimum coverage of two. We called haplogroups with HaploGrep2[47] based on phylotree[48] (mtDNA tree build 17 (accessed 18 February 2016)). Mutational differences, compared to the revised Cambridge Reference Sequence (GenBank reference sequence: NC_012920.1) and corresponding haplogroups, can be viewed in Supplementary Table 2. We computed haplogroup frequencies for relevant ancient populations (Supplementary Table 3) after removing close relatives with the same mtDNA.

Y-chromosome analysis. We determined Y-chromosome haplogroups for both new and published samples (Supplementary Information section 5). We made use of the sequences mapping to 1,240k Y-chromosome targets, restricting our analysis to sequences with mapping quality ≥ 30 and bases with quality ≥ 30. We called haplogroups by determining the most derived mutation for each sample, using the nomenclature of the International Society of Genetic Genealogy (http://www.isogg.org) version 11.110 (accessed 21 April 2016). Haplogroups and their supporting derived mutations can be viewed in Supplementary Table 4.

Merging newly generated data with published data. We assembled two datasets for genome-wide analyses. The first dataset is HO, which includes 2,572 present-day individuals from worldwide populations genotyped on the Human Origins Array[11,12,49] and 683 ancient individuals. The ancient set includes 211 Beaker-complex-associated individuals (195 newly reported, 7 with shotgun data[3] for which we generated 1,240k capture data and 9 that had previously been published[3,4]), 68 newly reported individuals from relevant ancient populations and 298 individuals that had previously been published[12,18,19,21–23,50–57] (Supplementary Table 1). We kept 591,642 autosomal SNPs after intersecting autosomal SNPs in the 1,240k capture with the analysis set of 594,924 SNPs from a previous publication[11]. The second dataset is HOIll, which includes the same set of ancient samples and 300 present-day individuals from 142 populations sequenced to high coverage as part of the Simons Genome Diversity Project[13]. For this dataset, we used 1,054,671 autosomal SNPs, excluding SNPs of the 1,240k array located on sex chromosomes or with known functional effects.

For each individual, we represented the allele at each SNP by randomly sampling one sequence and discarding the first and the last two nucleotides of each sequence.

Abbreviations. We have used the following abbreviations in population labels: E, Early; M, Middle; L, Late; N, Neolithic; CA, Copper Age; BA, Bronze Age; BC, Beaker complex; N_Iberia, northern Iberia; C_Iberia, central Iberia; SE_Iberia, southeast Iberia; and SW_Iberia, southwest Iberia.

Principal component analysis. We carried out principal component analysis on the HO dataset using the 'smartpca' program in EIGENSOFT[58]. We computed principal components on 990 present-day west Eurasians and projected ancient individuals using lsqproject:YES and shrinkmode:YES.

ADMIXTURE analysis. We performed model-based clustering analysis using ADMIXTURE[17] on the HO reference dataset, which included 2,572 present-day individuals from worldwide populations and the ancient individuals. First, we carried out linkage disequilibrium pruning on the dataset using PLINK[59] with the flag–indep-pairwise 200 25 0.4, leaving 306,393 SNPs. We ran ADMIXTURE with the cross validation (–cv.) flag specifying from $K=2$ to $K=20$ clusters, with 20 replicates for each value of K. For each value of K, the replicate with highest log likelihood was kept. In Extended Data Fig. 3b we show the cluster assignments at $K=8$ of newly reported individuals and other relevant ancient samples for comparison. We chose this value of K as it was the lowest one for which components of ancestry related both to Iranian Neolithic farmers and European Mesolithic hunter-gatherers were maximized.

***f*-statistics.** We computed *f*-statistics on the HOIll dataset using ADMIXTOOLS[49] with default parameters (Supplementary Information section 6). We used qpDstat with f4mode:Yes for f_4-statistics and qp3Pop for outgroup f_3-statistics. We computed standard errors using a weighted block jackknife[60] over 5-Mb blocks.

Inference of mixture proportions. We estimated ancestry proportions on the HOIll dataset using qpAdm[2] and a basic set of nine outgroups: Mota, Ust_Ishim, MA1, Villabruna, Mbuti, Papuan, Onge, Han and Karitiana. For some analyses (Supplementary Information section 8) we added additional outgroups to this basic set.

Admixture graph modelling. We modelled the relationships between populations in an Admixture Graph framework with the software qpGraph in ADMIXTOOLS[49], using the HOIll dataset and Mbuti as an outgroup (Supplementary Information section 7).

Allele frequency estimation from read counts. We used allele counts at each SNP to perform maximum likelihood estimations of allele frequencies in ancient populations as in ref. 4. In Extended Data Fig. 7, we show derived allele frequency estimates at three SNPs of functional importance for different ancient populations.

Data availability. All 1,240k and mitochondrial capture sequencing data are available from the European Nucleotide Archive, accession number PRJEB23635. The genotype dataset is available from the Reich Laboratory website at https://reich.hms.harvard.edu/datasets.

34. Dabney, J. *et al.* Complete mitochondrial genome sequence of a Middle Pleistocene cave bear reconstructed from ultrashort DNA fragments. *Proc. Natl Acad. Sci. USA* **110,** 15758–15763 (2013).
35. Damgaard, P. B. *et al.* Improving access to endogenous DNA in ancient bones and teeth. *Sci. Rep.* **5,** 11184 (2015).
36. Korlević, P. *et al.* Reducing microbial and human contamination in DNA extractions from ancient bones and teeth. *Biotechniques* **59,** 87–93 (2015).
37. Rohland, N., Harney, E., Mallick, S., Nordenfelt, S. & Reich, D. Partial uracil–DNA–glycosylase treatment for screening of ancient DNA. *Philos. Trans. R. Soc. Lond. B* **370,** 20130624 (2015).
38. Briggs, A. W. *et al.* Removal of deaminated cytosines and detection of *in vivo* methylation in ancient DNA. *Nucleic Acids Res.* **38,** e87 (2010).
39. Maricic, T., Whitten, M. & Pääbo, S. Multiplexed DNA sequence capture of mitochondrial genomes using PCR products. *PLoS ONE* **5,** e14004 (2010).
40. Kircher, M., Sawyer, S. & Meyer, M. Double indexing overcomes inaccuracies in multiplex sequencing on the Illumina platform. *Nucleic Acids Res.* **40,** e3 (2012).
41. Behar, D. M. *et al.* A 'Copernican' reassessment of the human mitochondrial DNA tree from its root. *Am. J. Hum. Genet.* **90,** 675–684 (2012).
42. Li, H. & Durbin, R. Fast and accurate short read alignment with Burrows–Wheeler transform. *Bioinformatics* **25,** 1754–1760 (2009).
43. Fu, Q. *et al.* A revised timescale for human evolution based on ancient mitochondrial genomes. *Curr. Biol.* **23,** 553–559 (2013).
44. Sawyer, S., Krause, J., Guschanski, K., Savolainen, V. & Pääbo, S. Temporal patterns of nucleotide misincorporations and DNA fragmentation in ancient DNA. *PLoS ONE* **7,** e34131 (2012).
45. Korneliussen, T. S., Albrechtsen, A. & Nielsen, R. ANGSD: analysis of next generation sequencing data. *BMC Bioinformatics* **15,** 356 (2014).
46. Li, H. *et al.* The sequence alignment/map format and SAMtools. *Bioinformatics* **25,** 2078–2079 (2009).
47. Weissensteiner, H. *et al.* HaploGrep 2: mitochondrial haplogroup classification in the era of high-throughput sequencing. *Nucleic Acids Res.* **44,** W58–W63 (2016).

48. van Oven, M. & Kayser, M. Updated comprehensive phylogenetic tree of global human mitochondrial DNA variation. *Hum. Mutat.* **30,** E386–E394 (2009).
49. Patterson, N. *et al.* Ancient admixture in human history. *Genetics* **192,** 1065–1093 (2012).
50. Raghavan, M. *et al.* Upper Palaeolithic Siberian genome reveals dual ancestry of Native Americans. *Nature* **505,** 87–91 (2014).
51. Omrak, A. *et al.* Genomic evidence establishes Anatolia as the source of the European Neolithic gene pool. *Curr. Biol.* **26,** 270–275 (2016).
52. Gallego Llorente, M. *et al.* Ancient Ethiopian genome reveals extensive Eurasian admixture in Eastern Africa. *Science* **350,** 820–822 (2015).
53. Fu, Q. *et al.* The genetic history of Ice Age Europe. *Nature* **534,** 200–205 (2016).
54. Kılınç, G. M. *et al.* The demographic development of the first farmers in Anatolia. *Curr. Biol.* **26,** 2659–2666 (2016).
55. Gallego-Llorente, M. *et al.* The genetics of an early Neolithic pastoralist from the Zagros, Iran. *Sci. Rep.* **6,** 31326 (2016).
56. Olalde, I. *et al.* Derived immune and ancestral pigmentation alleles in a 7,000-year-old Mesolithic European. *Nature* **507,** 225–228 (2014).
57. Hofmanová, Z. *et al.* Early farmers from across Europe directly descended from Neolithic Aegeans. *Proc. Natl Acad. Sci. USA* **113,** 6886–6891 (2016).
58. Patterson, N., Price, A. L. & Reich, D. Population structure and eigenanalysis. *PLoS Genet.* **2,** e190 (2006).
59. Purcell, S. *et al.* PLINK: a tool set for whole-genome association and population-based linkage analyses. *Am. J. Hum. Genet.* **81,** 559–575 (2007).
60. Busing, F. M. T. A., Meijer, E. & Van Der Leeden, R. Delete-m jackknife for unequal m. *Stat. Comput.* **9,** 3–8 (1999).
61. Rojo-Guerra, M. Á., Kunst, M., Garrido-Pena, R. & García-Martínez de Lagrán, I. & Morán-Dauchez, G. *Un desafío a la eternidad. Tumbas monumentales del Valle de Ambrona (Memorias Arqueología en Castilla y León 14)* (Junta de Castilla y León, 2005).
62. Gamba, C. *et al.* Genome flux and stasis in a five millennium transect of European prehistory. *Nat. Commun.* **5,** 5257 (2014).

Extended Data Figure 1 | Beaker-complex artefacts. a, 'All-Over-Cord' Beaker from Bathgate, West Lothian, Scotland. Photograph: © National Museums Scotland. **b**, Beaker-complex grave goods from La Sima III barrow, Soria, Spain[61]. The set includes Beaker pots of the so-called 'Maritime style'. Photograph: Junta de Castilla y León, Archivo Museo Numantino, Alejandro Plaza.

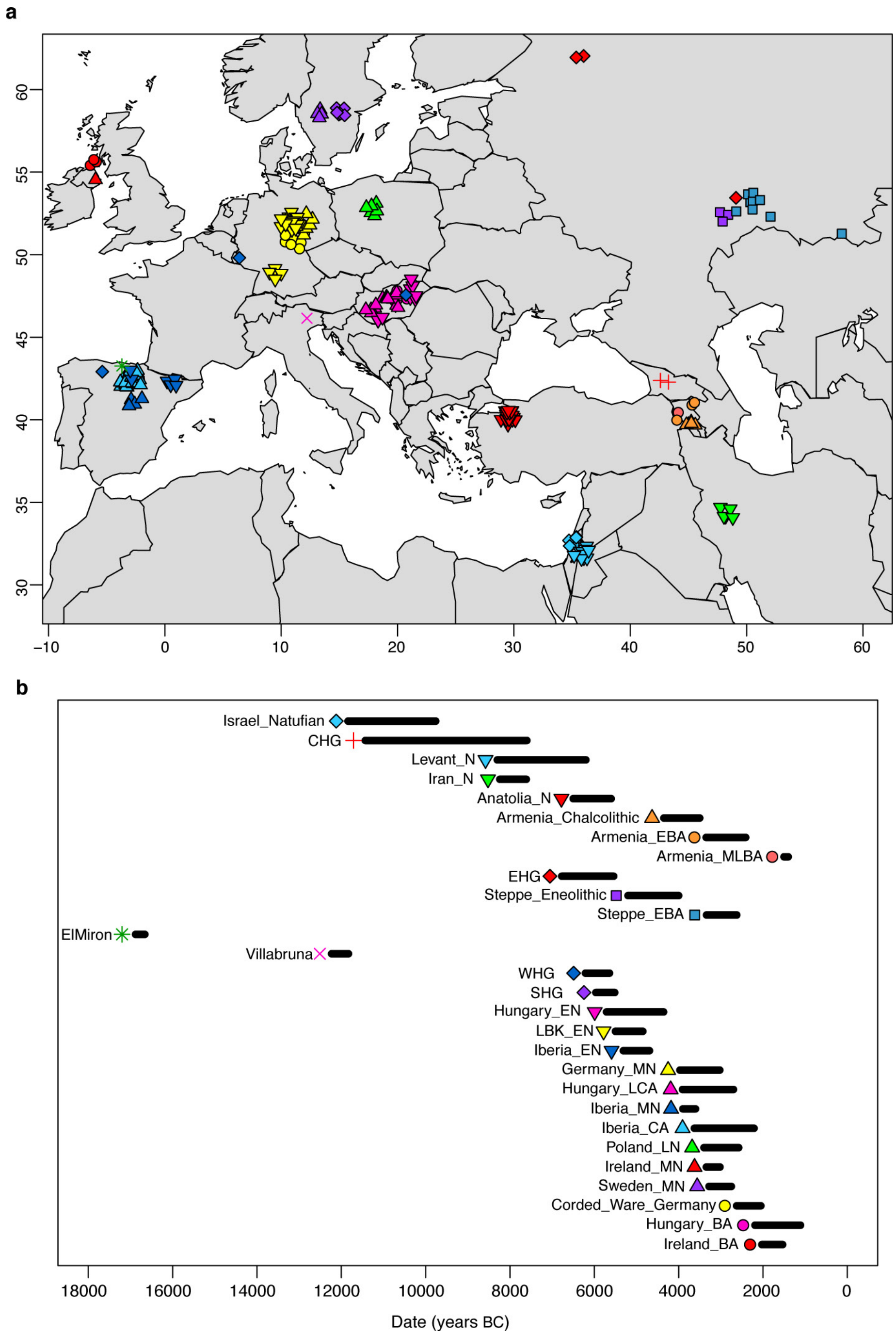

Extended Data Figure 2 | Ancient individuals with previously published genome-wide data used in this study. a, Sampling locations. **b**, Time ranges. WHG, western hunter-gatherers; EHG, eastern hunter-gatherers; SHG, Scandinavian hunter-gatherers; CHG, Caucasus hunter-gatherers; E, Early; M, Middle; L, Late; N, Neolithic; CA, Copper Age; and BA, Bronze Age. Map data from the R package 'maps'.

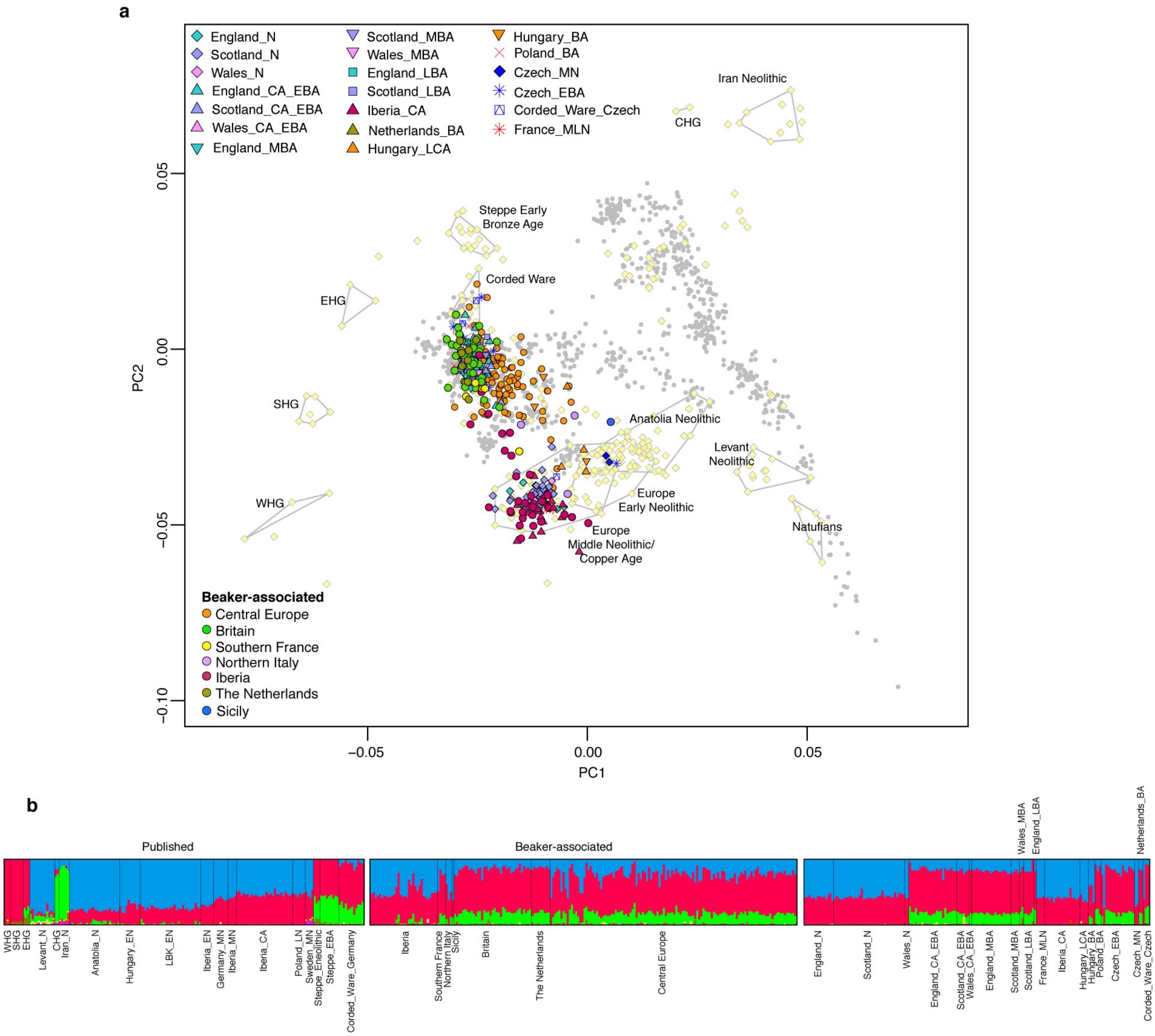

Extended Data Figure 3 | Population structure. a, Principal component analysis of 990 present-day west Eurasian individuals (grey dots), with previously published (pale yellow) and new ancient samples projected onto the first two principal components. **b**, ADMIXTURE clustering analysis with $K = 8$ showing ancient individuals. WHG, western hunter-gatherers; EHG, eastern hunter-gatherers; SHG, Scandinavian hunter-gatherers; CHG, Caucasus hunter-gatherers; E, Early; M, Middle; L, Late; N, Neolithic; CA, Copper Age; and BA, Bronze Age.

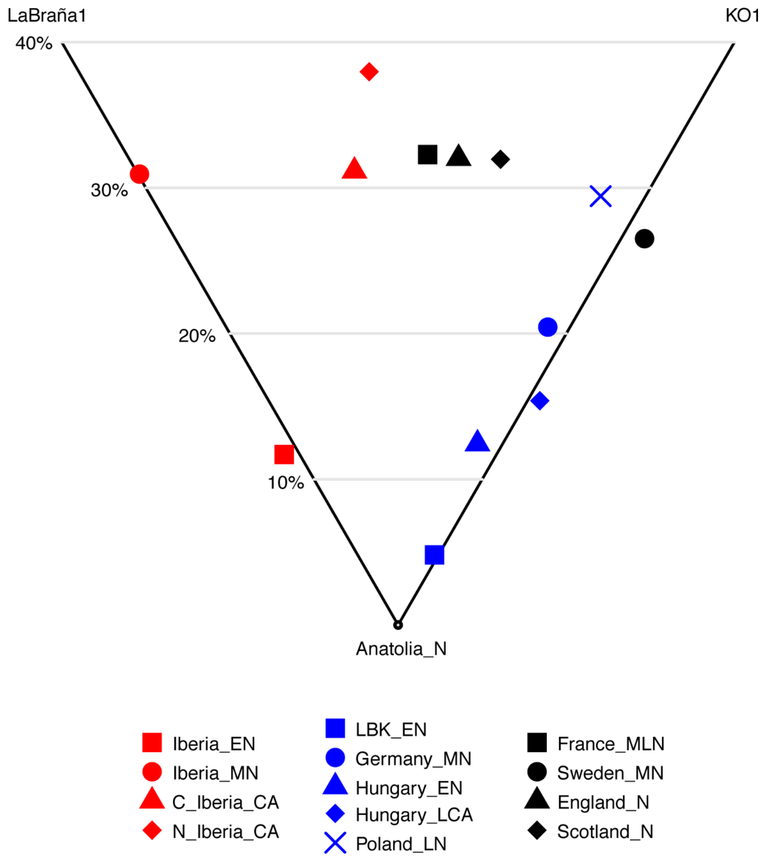

Extended Data Figure 4 | Hunter-gatherer affinities in Neolithic and Copper Age Europe. Differential affinity to hunter-gatherer individuals (La Braña1[56] from Spain and KO1[62] from Hungary) in European populations before the emergence of the Beaker complex. See Supplementary Information section 8 for mixture proportions and standard errors computed with qpAdm[2]. E, Early; M, Middle; L, Late; N, Neolithic; CA, Copper Age; BA, Bronze Age; N_Iberia, northern Iberia; and C_Iberia, central Iberia.

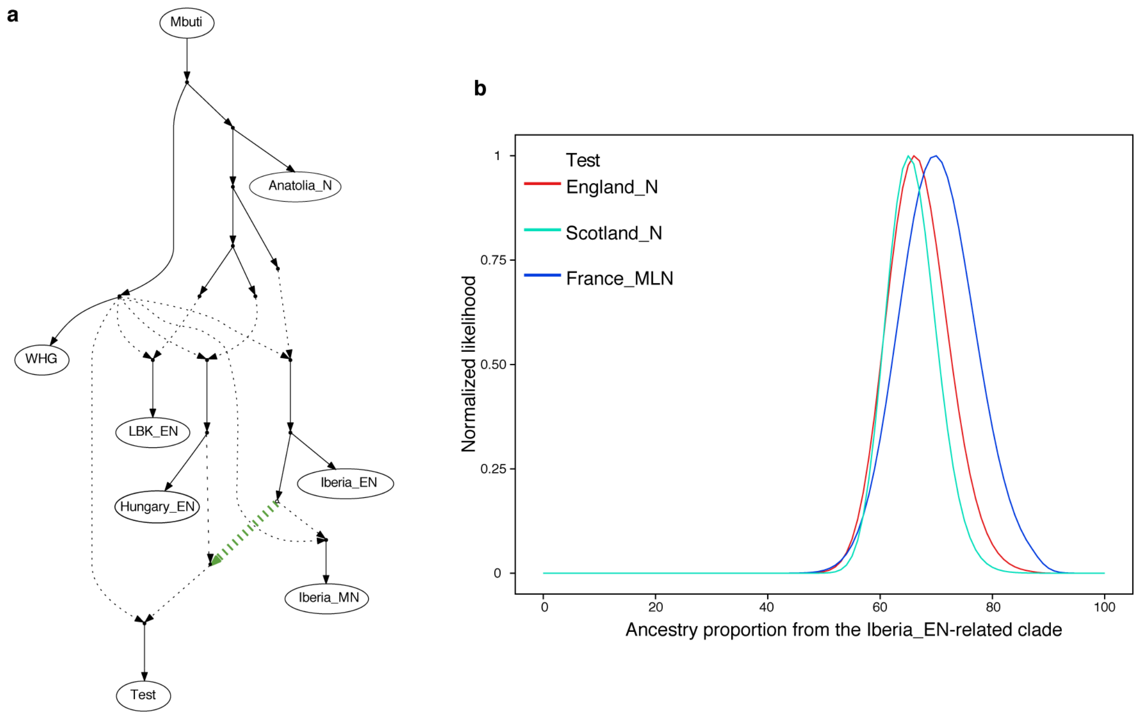

Extended Data Figure 5 | Modelling the relationships between Neolithic populations. a, Admixture graph fitting a test population as a mixture of sources related to both Iberia_EN and Hungary_EN. **b**, Likelihood distribution for models with different proportions of the source related to Iberia_EN (green admixture edge in **a**) when the test population is England_N, Scotland_N or France_MLN. E, Early; M, Middle; L, Late; and N, Neolithic.

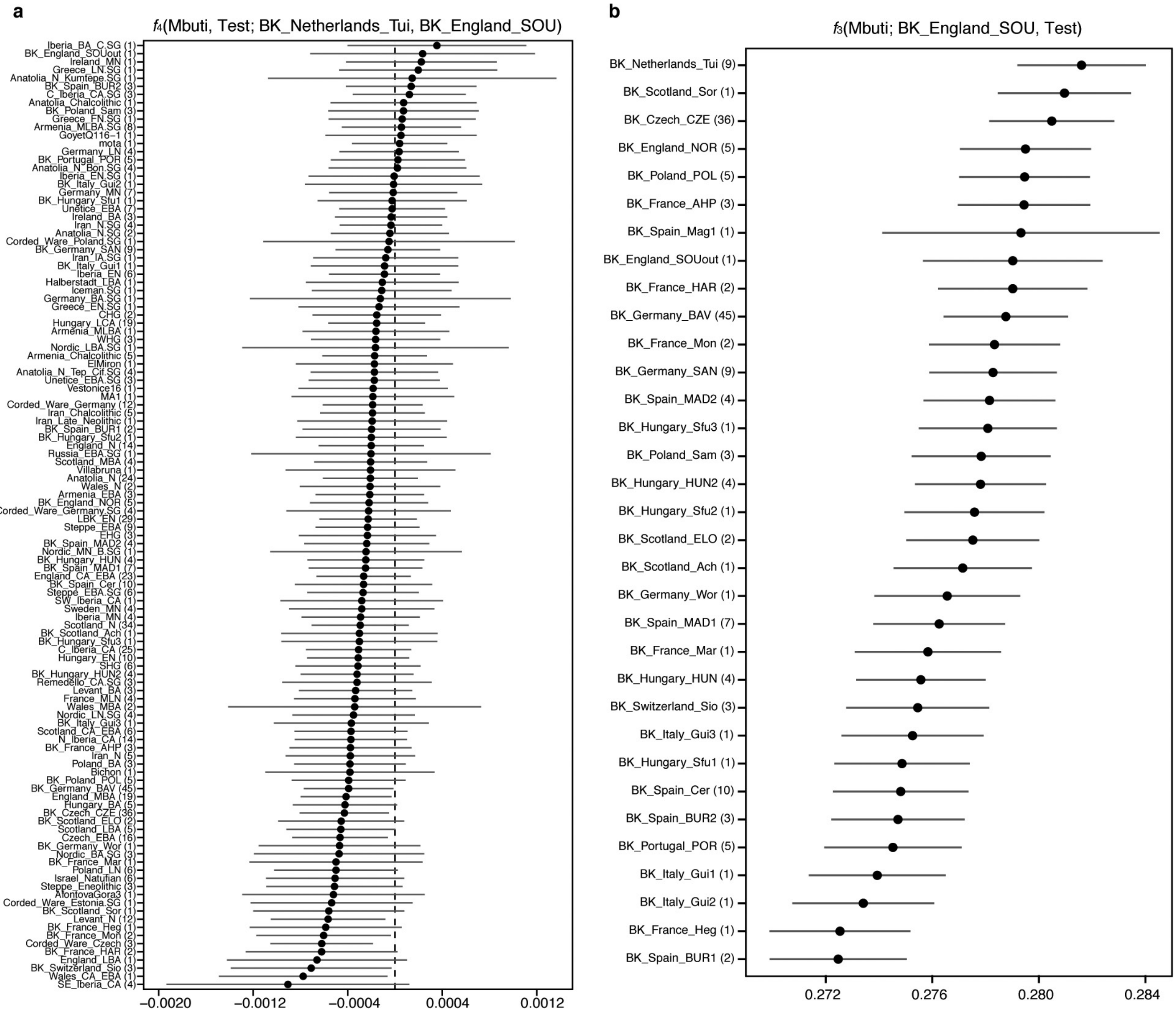

Extended Data Figure 6 | Genetic affinity between Beaker-complex-associated individuals from southern England and the Netherlands. **a**, *f*-statistics of the form f_4(Mbuti, test; BK_Netherlands_Tui, BK_England_SOU). Negative values indicate that test population is closer to BK_Netherlands_Tui than to BK_England_SOU; positive values indicate that the test population is closer to BK_England_SOU than to BK_Netherlands_Tui. Error bars represent ± 3 standard errors. **b**, Outgroup f_3-statistics of the form f_3(Mbuti; BK_England_SOU, test) measuring shared genetic drift between BK_England_SOU and other Beaker-complex-associated groups. Error bars represent ± 1 standard errors. Number of individuals for each group is given in parentheses. BK_Netherlands_Tui, Beaker-complex-associated individuals from De Tuithoorn (Oostwoud, the Netherlands); BK_England_SOU, Beaker-complex-associated individuals from southern England. See Supplementary Table 1 for individuals associated with each population label.

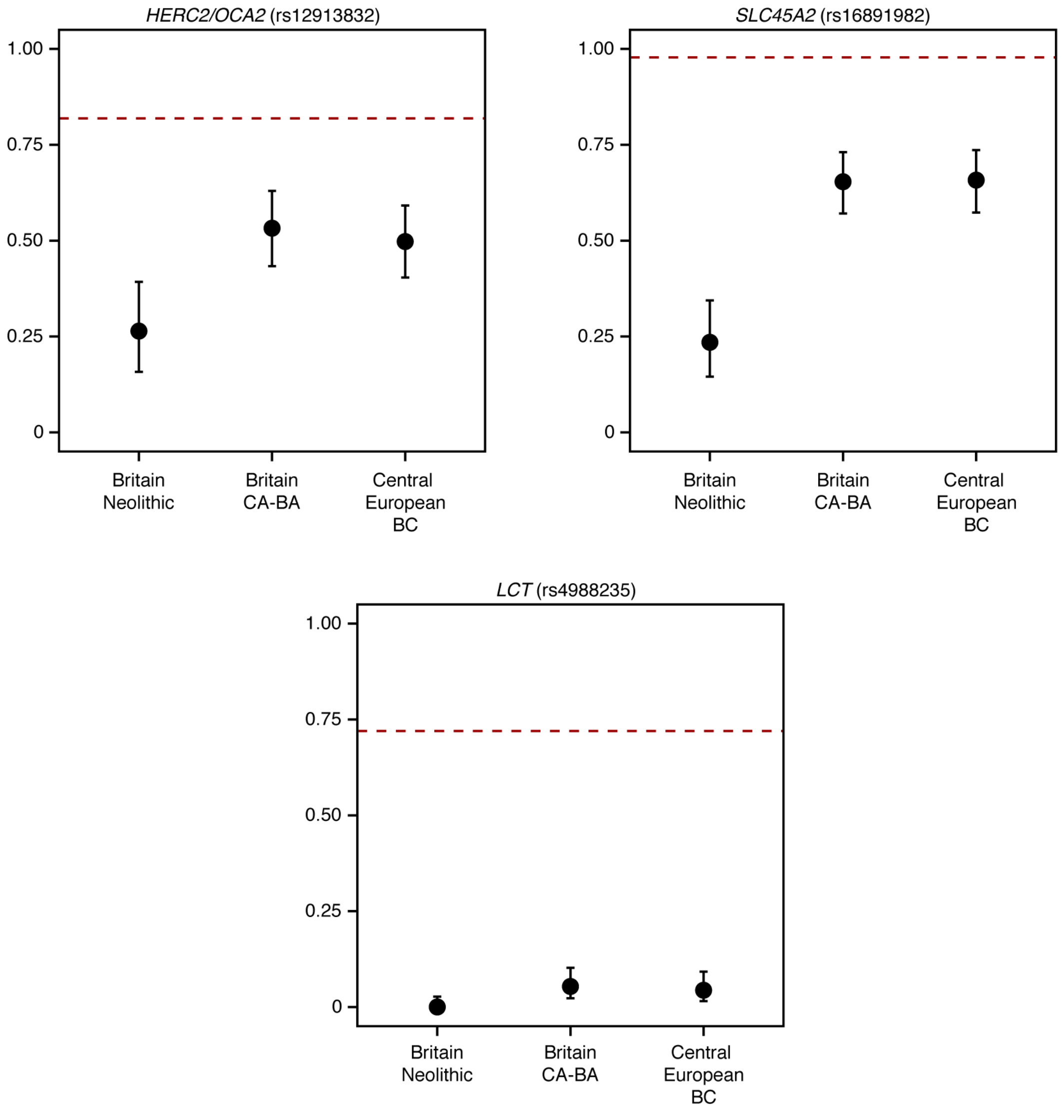

Extended Data Figure 7 | Derived allele frequencies at three SNPs of functional importance. Error bars represent 1.9-log-likelihood support interval. The red dashed lines show allele frequencies in the 1000 Genomes Project (http://www.internationalgenome.org/) 'GBR' population (present-day people from Great Britain). Sample sizes are 50, 98 and 117 for Britain Neolithic, Britain Copper Age and Bronze Age, and central European Beaker-complex-associated individuals, respectively. BC, Beaker complex; CA, Copper Age; and BA, Bronze Age.

Extended Data Table 1 | Sites from outside Britain with new genome-wide data reported in this study

Site	N	Approx. date range (BC)	Country
Brandysek	12	2900–2200	Czech Republic
Kněževes	2	2500–1900	Czech Republic
Lochenice	1	2500–1900	Czech Republic
Lovosice II	1	2500–1900	Czech Republic
Moravská Nová Ves	4	2300–1900	Czech Republic
Prague 5 - Malá Ohrada	1	2500–2200	Czech Republic
Prague 5, Jinonice	14	2200–1700	Czech Republic
Prague 8, Kobylisy, Ke Stírce Street	12	2500–1900	Czech Republic
Radovesice	13	2500–2200	Czech Republic
Velké Přílepy	3	2500–1900	Czech Republic
Clos de Roque, Saint Maximin-la-Sainte-Baume	3	4700–4500	France
Collet Redon, La Couronne-Martigues	1	3500–3100	France
Hégenheim Necropole, Haut-Rhin	1	2800–2500	France
La Fare, Forcalquier	1	2500–2200	France
Marlens, Sur les Barmes, Haute-Savoie	1	2500–2100	France
Mondelange, PAC de la Sente, Moselle	2	2400–1900	France
Rouffach, Haut-Rhin	1	2300–2100	France
Sierentz, Les Villas d'Aurele, Haut-Rhin	2	2600–2300	France
Villard, Lauzet-Ubaye	2	2200–1900	France
Alburg-Lerchenhaid, Spedition Häring, Bavaria	13	2500–2100	Germany
Augsburg Sportgelände, Augsburg, Bavaria	6	2500–2000	Germany
Hugo-Eckener-Straße, Augsburg, Bavaria	3	2500–2000	Germany
Irlbach, County of Straubing-Bogen, Bavaria	17	2500–2000	Germany
Künzing-Bruck, Lkr. Deggendorf, Bavaria	3	2500–2000	Germany
Landau an der Isar, Bavaria	5	2500–2000	Germany
Manching-Oberstimm, Bavaria	2	2500–2000	Germany
Osterhofen-Altenmarkt, Bavaria	4	2600–2000	Germany
Unterer Talweg 58-62, Augsburg, Bavaria	2	2500–2200	Germany
Unterer Talweg 85, Augsburg, Bavaria	1	2400–2100	Germany
Weichering, Bavaria	4	2500–2000	Germany
Worms-Herrnsheim, Rhineland-Palatinate	1	2500–2000	Germany
Budakalász, Csajerszke (M0 Site 12)	2	2600–2200	Hungary
Budapest-Békásmegyer	3	2500–2100	Hungary
Mezőcsát-Hörcsögös	4	3400–3000	Hungary
Szigetszentmiklós-Üdülősor	4	2500–2200	Hungary
Szigetszentmiklós,Felső Ürge-hegyi dűlő	6	2500–2200	Hungary
Pergole 2, Partanna, Sicily	3	2500–1900	Italy
Via Guidorossi, Parma, Emilia Romagna	3	2200–1900	Italy
Dzielnica	1	2300–2000	Poland
Iwiny	1	2300–2000	Poland
Jordanów Śląski	1	2300–2200	Poland
Kornice	4	2500–2100	Poland
Racibórz-Stara Wieś	1	2300–2000	Poland
Samborzec	3	2500–2100	Poland
Strachów	1	2000–1800	Poland
Żerniki Wielkie	1	2300–2100	Poland
Bolores, Estremadura	1	2800–2600	Portugal
Cova da Moura, Torres Vedras	1	2300–2100	Portugal
Galeria da Cisterna, Almonda	2	2500–2200	Portugal
Verdelha dos Ruivos, District of Lisbon	3	2700–2300	Portugal
Arroyal I, Burgos	5	2600–2200	Spain
Camino de las Yeseras, Madrid	14	2800–1700	Spain
Camino del Molino, Caravaca, Murcia	4	2900–2100	Spain
Humanejos, Madrid	11	2900–2000	Spain
La Magdalena, Madrid	3	2500–2000	Spain
Paris Street, Cerdanyola, Barcelona	10	2900–2300	Spain
Virgazal, Tablada de Rudrón, Burgos	1	2300–2000	Spain
Sion-Petit-Chasseur, Dolmen XI	3	2500–2000	Switzerland
De Tuithoorn, Oostwoud, Noord-Holland	11	2600–1600	The Netherlands

Extended Data Table 2 | Sites from Britain with new genome-wide data reported in this study

Site	N	Approx. date range (BC)	Country
Abingdon Spring Road cemetery, Oxfordshire, England	1	2500–2200	Great Britain
Amesbury Down, Wiltshire, England	13	2500–1300	Great Britain
Banbury Lane, Northamptonshire, England	3	3400–3100	Great Britain
Barrow Hills, Radley, Oxfordshire, England	1	2300–1800	Great Britain
Barton Stacey, Hampshire, England	1	2200–2000	Great Britain
Baston and Langtoft, South Lincolnshire, England	2	1700–1600	Great Britain
Biddenham Loop, Bedfordshire, England	9	1600–1300	Great Britain
Boscombe Airfield, Wiltshire, England	1	1800–1600	Great Britain
Canada Farm, Sixpenny Handley, Dorset, England	2	2500–2300	Great Britain
Carsington Pasture Cave, Derbyshire, England	2	3700–2000	Great Britain
Central Flying School, Upavon, Wiltshire, England	1	2500–1800	Great Britain
Cissbury Flint Mine, Worthing, West Sussex, England	1	3600–3400	Great Britain
Clay Farm, Cambridgeshire, England	2	1400–1300	Great Britain
Dairy Farm, Willington, England	1	2300–1900	Great Britain
Ditchling Road, Brighton, Sussex, England	1	2500–1900	Great Britain
Eton Rowing Course, Buckinghamshire, England	2	3600–2900	Great Britain
Flying School, Netheravon, Wiltshire, England	2	2500–1800	Great Britain
Fussell's Lodge, Salisbury, Wiltshire, England	2	3800–3600	Great Britain
Lesser Kelco Cave, Giggleswick Scar, North Yorkshire, England	1	3700–3500	Great Britain
Hasting Hill, Sunderland, Tyne and Wear, England	2	2500–1800	Great Britain
Hexham Golf Course, Northumberland, England	1	2000–1800	Great Britain
Low Hauxley, Northumberland, England	2	2100–1600	Great Britain
Melton Quarry, East Riding of Yorkshire, England	1	1900–1700	Great Britain
Neale's Cave, Paington, Devon, England	1	2000–1600	Great Britain
Nr. Ablington, Figheldean, England	1	2500–1800	Great Britain
Nr. Millbarrow, Wiltshire, England	1	3600–3400	Great Britain
Over Narrows, Needingworth Quarry, England	5	2200–1300	Great Britain
Porton Down, Wiltshire, England	2	2500–1900	Great Britain
Raven Scar Cave, Ingleton, North Yorkshire, England	1	1100–900	Great Britain
Reaverhill, Barrasford, Northumberland, England	1	2100–2000	Great Britain
River Thames, Mortlake/Syon Reach, London, England	2	2500–1700	Great Britain
Staxton Beacon, Staxton, England	1	2400–1600	Great Britain
Summerhill,Blaydon, Tyne and Wear, England	1	1900–1700	Great Britain
East Kent Access (Phase II), Thanet, Kent, England	4	2100–1700	Great Britain
Totty Pot, Cheddar, Somerset, England	1	2800–2500	Great Britain
Trumpington Meadows, Cambridge, England	2	2200–2000	Great Britain
Turners Yard, Fordham, Cambridgeshire, England	1	1700–1500	Great Britain
Upper Swell, Chipping Norton, Gloucestershire, England	1	4000–3300	Great Britain
Waterhall Farm, Chippenham, Cambridgeshire, England	1	2000–1700	Great Britain
West Deeping, Lincolnshire, England	1	2300–2000	Great Britain
Whitehawk, Brighton, Sussex, England	1	3700–3400	Great Britain
Wick Barrow, Stogursey, Somerset, England	1	2400–2000	Great Britain
Wilsford Down, Wilsford-cum-Lake, Wiltshire, England	2	2400–2000	Great Britain
Windmill Fields, Stockton-on-Tees, North Yorkshire,England	4	2300–2000	Great Britain
Yarnton, Oxfordshire, England	4	2500–1900	Great Britain
Aberdour Road, Dunfermline, Fife, Scotland	1	2000–1800	Great Britain
Achavanich, Wick, Highland, Scotland	1	2500–2100	Great Britain
Boatbridge Quarry, Thankerton, Scotland	1	2400–2100	Great Britain
Clachaig, Arran, North Ayrshire, Scotland	1	3500–3400	Great Britain
Covesea Cave 2, Moray, Scotland	3	2100–800	Great Britain
Covesea Caves, Moray, Scotland	2	1000–800	Great Britain
Distillery Cave, Oban, Argyll and Bute, Scotland	3	3800–3400	Great Britain
Doune, Perth and Kinross, Scotland	1	1800–1600	Great Britain
Dryburn Bridge, East Lothian, Scotland	2	2300–1900	Great Britain
Eweford Cottages, East Lothian, Scotland	1	2100–1900	Great Britain
Holm of Papa Westray North, Orkney, Scotland	4	3500–3100	Great Britain
Isbister, Orkney, Scotland	10	3300–2300	Great Britain
Leith, Merrilees Close, City of Edinburgh, Scotland	2	1600–1500	Great Britain
Longniddry, Evergreen House, Coast Road, East Lothian, Scotlan	3	1500–1300	Great Britain
Longniddry, Grainfoot, East Lothian, Scotland	1	1300–1000	Great Britain
Macarthur Cave, Oban, Argyll and Bute, Scotland	1	4000–3800	Great Britain
Pabay Mor, Lewis, Western Isles, Scotland	1	1400–1300	Great Britain
Point of Cott, Orkney, Scotland	2	3700–3100	Great Britain
Quoyness, Orkney, Scotland	1	3100–2900	Great Britain
Raschoille Cave, Oban, Argyll and Bute, Scotland	9	4000–2900	Great Britain
Sorisdale, Coll, Argyll and Bute, Scotland	1	2500–2100	Great Britain
Stenchme, Lop Ness, Orkney, Scotland	1	2000–1500	Great Britain
Thurston Mains, Innerwick, East Lothian, Scotland	1	2300–2000	Great Britain
Tulach an t'Sionnach, Highland, Scotland	1	3700–3500	Great Britain
Tulloch of Assery A, Highland, Scotland	1	3700–3400	Great Britain
Tulloch of Assery B, Highland, Scotland	1	3800–3600	Great Britain
Unstan, Orkney, Scotland	1	3400–3100	Great Britain
Culver Hole Cave, Port Eynon, West Glamorgan, Wales	1	1600–800	Great Britain
Great Orme Mines, Llandudno, North Wales	1	1700–1600	Great Britain
North Face Cave, Llandudno, North Wales	1	1400–1200	Great Britain
Rhos Ddigre, Llanarmon-yn-Iâl, Denbighshire, Wales	1	3100–2900	Great Britain
Tinkinswood, Cardiff, Glamorgan, Wales	1	3800–3600	Great Britain

Extended Data Table 3 | 111 newly reported radiocarbon dates

Sample	Date	Location	Country
I5024	2278–2032 calBC (3740±35 BP, Poz-84460)	Kněževes	Czech Republic
I4946	2296–2146 calBC (3805±20 BP, PSUAMS-2801)	Prague 5, Jinonice, Butovická Street	Czech Republic
I4895	2273–2047 calBC (3750±20 BP, PSUAMS-2852)	Prague 5, Jinonice, Butovická Street	Czech Republic
I4896	2288–2142 calBC (3785±20 BP, PSUAMS-2853)	Prague 5, Jinonice, Butovická Street	Czech Republic
I4884	1882–1745 calBC (3480±20 BP, PSUAMS-2842)	Prague 8, Kobylisy, Ke Stírce Street	Czech Republic
I4885	2289–2143 calBC (3790±20 BP, PSUAMS-2843)	Prague 8, Kobylisy, Ke Stírce Street	Czech Republic
I4886	2205–2042 calBC (3740±20 BP, PSUAMS-2844)	Prague 8, Kobylisy, Ke Stírce Street	Czech Republic
I4887	2201–2039 calBC (3730±20 BP, PSUAMS-2845)	Prague 8, Kobylisy, Ke Stírce Street	Czech Republic
I4888	2190–2029 calBC (3700±20 BP, PSUAMS-2846)	Prague 8, Kobylisy, Ke Stírce Street	Czech Republic
I4889	2281–2062 calBC (3765±20 BP, PSUAMS-2847)	Prague 8, Kobylisy, Ke Stírce Street	Czech Republic
I4891	2281–2062 calBC (3765±20 BP, PSUAMS-2848)	Prague 8, Kobylisy, Ke Stírce Street	Czech Republic
I4892	1881–1701 calBC (3475±20 BP, PSUAMS-2849)	Prague 8, Kobylisy, Ke Stírce Street	Czech Republic
I4893	4449–4348 calBC (5550±20 BP, PSUAMS-2850)	Prague 8, Kobylisy, Ke Stírce Street	Czech Republic
I4894	4488–4368 calBC (5610±20 BP, PSUAMS-2851)	Prague 8, Kobylisy, Ke Stírce Street	Czech Republic
I4945	2291–2144 calBC (3795±20 BP, PSUAMS-2854)	Prague 8, Kobylisy, Ke Stírce Street	Czech Republic
I4305	4825–4616 calBC (5860±35 BP, PSUAMS-2225)	Clos de Roque, Saint Maximin-la-Sainte-Baume	France
I4304	4787–4589 calBC (5830±35 BP, PSUAMS-2226)	Clos de Roque, Saint Maximin-la-Sainte-Baume	France
I4303	4778–4586 calBC (5820±30 BP, PSUAMS-2260)	Clos de Roque, Saint Maximin-la-Sainte-Baume	France
I1392	2833–2475 calBC (4047±29 BP, MAMS-25935)	Hégenheim Necropole, Haut-Rhin	France
I3875	2133–1946 calBC (3655±25 BP, PSUAMS-1834)	Villard, Lauzet-Ubaye	France
I3874	2200–2035 calBC (3725±25 BP, PSUAMS-1835)	Villard, Lauzet-Ubaye	France
I3593	2397–2145 calBC (3817±26 BP, BRAMS-1215)	Alburg-Lerchenhaid, Spedition Häring, Stkr. Straubing, Bavaria	Germany
I3590	2335–2140 calBC (3802±26 BP, BRAMS-1217)	Alburg-Lerchenhaid, Spedition Häring, Stkr. Straubing, Bavaria	Germany
I3592	2457–2203 calBC (3844±33 BP, BRAMS-1218)	Alburg-Lerchenhaid, Spedition Häring, Stkr. Straubing, Bavaria	Germany
I5017	2460–2206 calBC (3855±35 BP, Poz-84458)	Augsburg Sportgelände, Augsburg, Bavaria	Germany
I4250	2433–2149 calBC (3825±26 BP, BRAMS-1219)	Irlbach, County of Straubing-Bogen, Bavaria	Germany
I5021	2571–2341 calBC (3955±35 BP, Poz-84553)	Osterhofen-Altenmarkt, Bavaria	Germany
E09537_d	2471–2298 calBC (3909±29 BP, MAMS-29074)	Unterer Talweg 58-62, Augsburg, Bavaria	Germany
E09538	2464–2210 calBC (3870±30 BP, MAMS-29075)	Unterer Talweg 58-62, Augsburg, Bavaria	Germany
I5385	2455–2147 calBC (3827±33 BP, SUERC-71005)	Achavanich, Wick, Highland, Scotland	Great Britain
I2457	2199–2030 calBC (3717±28 BP, SUERC-69975)	Amesbury Down, Wiltshire, England	Great Britain
I2416	2455–2151 calBC (3830±30 BP, Beta-432804)	Amesbury Down, Wiltshire, England	Great Britain
I2596	2273–2034 calBC (3739±30 BP, NZA-32484)	Amesbury Down, Wiltshire, England	Great Britain
I2566	2204–2035 calBC (3734±25 BP, NZA-32490)	Amesbury Down, Wiltshire, England	Great Britain
I2598	2135–1953 calBC (3664±30 BP, NZA-32494)	Amesbury Down, Wiltshire, England	Great Britain
I2418	2455–2200 calBC (3836±25 BP, NZA-32788)	Amesbury Down, Wiltshire, England	Great Britain
I2565	2457–2147 calBC (3829±38 BP, OxA-13562)	Amesbury Down, Wiltshire, England	Great Britain
I2457	2467–2290 calBC (3890±30 BP, SUERC-36210)	Amesbury Down, Wiltshire, England	Great Britain
I2460	2022–1827 calBC (3575±27 BP, SUERC-53041)	Amesbury Down, Wiltshire, England	Great Britain
I2459	2455–2150 calBC (3829±30 BP, SUERC-54823)	Amesbury Down, Wiltshire, England	Great Britain
I5373	2194–1980 calBC (3694±25 BP, BRAMS-1230)	Carsington Pasture Cave, Brassington, Derbyshire, England	Great Britain
I2988	3516–3361 calBC (4645±29 BP, SUERC-68711)	Clachaig, Arran, North Ayrshire, Scotland	Great Britain
I2860	969–815 calBC (2738±29 BP, SUERC-68715)	Covesea Cave 2, Moray, Scotland	Great Britain
I2861	976–828 calBC (2757±29 BP, SUERC-68716)	Covesea Cave 2, Moray, Scotland	Great Britain
I3132	2118–1887 calBC (3614±33 BP, SUERC-69070)	Covesea Cave 2, Moray, Scotland	Great Britain
I3130	977–829 calBC (2758±29 BP, SUERC-68713)	Covesea Caves, Moray, Scotland	Great Britain
I2859	910–809 calBC (2714±29 BP, SUERC-68714)	Covesea Caves, Moray, Scotland	Great Britain
I2452	2198–1980 calBC (3700±30 BP, Beta-444979)	Dairy Farm, Willington, England	Great Britain
I2452	2276–2029 calBC (3735±35 BP, Poz-83405)	Dairy Farm, Willington, England	Great Britain
I2659	3761–3643 calBC (4914±27 BP, SUERC-68702)	Distillery Cave, Oban, Argyll and Bute, Scotland	Great Britain
I2660	3513–3352 calBC (4631±29 BP, SUERC-68703)	Distillery Cave, Oban, Argyll and Bute, Scotland	Great Britain
I2691	3700–3639 calBC (4881±25 BP, SUERC-68704)	Distillery Cave, Oban, Argyll and Bute, Scotland	Great Britain
I6774	2287–2044 calBC (3760±30 BP, SUERC-74755)	Ditchling Road, Brighton, Sussex, England	Great Britain
I2605	3631–3372 calBC (4710±35 BP, Poz-83483)	Eton Rowing Course, Buckinghamshire, England	Great Britain
I1775	1730–1532 calBC (3344±27 BP, OxA-14308)	Great Orme, Llandudno, North Wales	Great Britain
I2574	1414–1227 calBC (3065±36 BP, SUERC-62072)	Great Orme, Llandudno, North Wales	Great Britain
I2612	2464–2208 calBC (3865±35 BP, Poz-83492)	Hasting Hill, Sunderland, Tyne and Wear, England	Great Britain
I2609	2022–1771 calBC (3560±40 BP, Poz-83423)	Hexham Golf Course, Northumberland, England	Great Britain
I2636	3519–3361 calBC (4651±33 BP, SUERC-68640)	Holm of Papa Westray North, Orkney, Scotland	Great Britain
I2637	3629–3370 calBC (4697±33 BP, SUERC-68641)	Holm of Papa Westray North, Orkney, Scotland	Great Britain
I2650	3638–3380 calBC (4754±36 BP, SUERC-68642)	Holm of Papa Westray North, Orkney, Scotland	Great Britain
I2651	3360–3098 calBC (4525±36 BP, SUERC-68643)	Holm of Papa Westray North, Orkney, Scotland	Great Britain
I2630	2580–2463 calBC (3999±32 BP, SUERC-68632)	Isbister, Orkney, Scotland	Great Britain
I2932	2570–2347 calBC (3962±29 BP, SUERC-68721)	Isbister, Orkney, Scotland	Great Britain
I2933	3010–2885 calBC (4309±29 BP, SUERC-68722)	Isbister, Orkney, Scotland	Great Britain
I2935	3335–3011 calBC (4451±29 BP, SUERC-68723)	Isbister, Orkney, Scotland	Great Britain
I3085	3338–3026 calBC (4471±29 BP, SUERC-68724)	Isbister, Orkney, Scotland	Great Britain
I2978	3335–3023 calBC (4464±29 BP, SUERC-68725)	Isbister, Orkney, Scotland	Great Britain
I2979	3333–2941 calBC (4447±29 BP, SUERC-68726)	Isbister, Orkney, Scotland	Great Britain
I2934	3338–3022 calBC (4466±33 BP, SUERC-69071)	Isbister, Orkney, Scotland	Great Britain
I2977	3008–2763 calBC (4275±33 BP, SUERC-69072)	Isbister, Orkney, Scotland	Great Britain
I2657	3951–3780 calBC (5052±30 BP, SUERC-68701)	Macarthur Cave, Oban, Argyll and Bute, Scotland	Great Britain
I5441	1938–1744 calBC (3512±37 BP, OxA-16522)	Neale's Cave, Paignton, Devon, England	Great Britain
I4949	3629–3376 calBC (4715±20 BP, PSUAMS-2513)	Nr. Millbarrow, Winterbourne Monkton, Wiltshire, England	Great Britain
I2980	3360–3101 calBC (4530±33 BP, SUERC-69073)	Point of Cott, Orkney, Scotland	Great Britain
I2796	3705–3535 calBC (4856±33 BP, SUERC-69074)	Point of Cott, Orkney, Scotland	Great Britain
I2631	3097–2906 calBC (4384±36 BP, SUERC-68633)	Quoyness, Orkney, Scotland	Great Britain
I3135	3640–3383 calBC (4770±30 BP, PSUAMS-2068)	Raschoille Cave, Oban, Argyll and Bute, Scotland	Great Britain
I3136	3520–3365 calBC (4665±30 BP, PSUAMS-2069)	Raschoille Cave, Oban, Argyll and Bute, Scotland	Great Britain
I3133	3631–3377 calBC (4725±20 BP, PSUAMS-2154)	Raschoille Cave, Oban, Argyll and Bute, Scotland	Great Britain
I3134	3633–3377 calBC (4730±25 BP, PSUAMS-2155)	Raschoille Cave, Oban, Argyll and Bute, Scotland	Great Britain
I3138	3263–2923 calBC (4415±25 BP, PSUAMS-2156)	Raschoille Cave, Oban, Argyll and Bute, Scotland	Great Britain
I2610	1935–1745 calBC (3515±35 BP, Poz-83498)	Summerhill, Blaydon, Tyne and Wear, England	Great Britain
I2634	3703–3534 calBC (4851±34 BP, SUERC-68638)	Tulach an t'Sionnach, Highland, Scotland	Great Britain
I2635	3652–3389 calBC (4796±37 BP, SUERC-68639)	Tulloch of Assery A, Highland, Scotland	Great Britain
I2633	3765–3641 calBC (4911±32 BP, SUERC-68634)	Tulloch of Assery B, Highland, Scotland	Great Britain
I2453	2288–2040 calBC (3760±35 BP, Poz-83404)	West Deeping, Lincolnshire, England	Great Britain
I2445	2136–1929 calBC (3650±35 BP, Poz-83407)	Yarnton, Oxfordshire, England	Great Britain
I2447	2115–1910 calBC (3625±25 BP, PSUAMS-2336)	Yarnton, Oxfordshire, England	Great Britain
I2786	2458–2205 calBC (3850±35 BP, Poz-83639)	Szigetszentmiklós-Felső-Urge hegyi dűlő	Hungary
I2787	2457–2201 calBC (3840±35 BP, Poz-83640)	Szigetszentmiklós-Felső-Urge hegyi dűlő	Hungary
I2741	2457–2153 calBC (3835±35 BP, Poz-83641)	Szigetszentmiklós-Felső-Urge hegyi dűlő	Hungary
I6531	2286–2038 calBC (3755±35 BP, Poz-86947)	Dzielnica	Poland
I6579	2335–2046 calBC (3780±35 BP, Poz-75954)	Iwiny	Poland
I6534	2456–2149 calBC (3830±35 BP, Poz-75936)	Kornice	Poland
I6582	2343–2057 calBC (3790±35 BP, Poz-75951)	Kornice	Poland
I4251	2431–2150 calBC (3825±25 BP, PSUAMS-2321)	Samborzec 1	Poland
I4252	2285–2138 calBC (3780±20 BP, PSUAMS-2338)	Samborzec 1	Poland
I4253	2456–2207 calBC (3850±20 BP, PSUAMS-2339)	Samborzec 1	Poland
I6538	2008–1765 calBC (3545±35 BP, Poz-86950)	Strachów	Poland
I6583	2289–2050 calBC (3770±30 BP, Poz-65207)	Zerniki Wielkie	Poland
I4229	2288–2134 calBC (3775±25 BP, PSUAMS-1750)	Cova da Moura	Portugal
I0462	2566–2345 calBC (3950±26 BP, MAMS-25936)	Arroyal I, Burgos	Spain
I4247	2464–2210 calBC (3870±30 BP, PSUAMS-2120)	Camino de las Yeseras, Madrid	Spain
I4245	2460–2291 calBC (3875±20 BP, PSUAMS-2320)	Camino de las Yeseras, Madrid	Spain
I0257	2572–2348 calBC (3965±29 BP, MAMS-25937)	Paris Street, Cerdanyola, Barcelona	Spain
I0825	2474–2298 calBC (3915±29 BP, MAMS-25939)	Paris Street, Cerdanyola, Barcelona	Spain
I0826	2834–2482 calBC (4051±28 BP, MAMS-25940)	Paris Street, Cerdanyola, Barcelona	Spain
I4068	2131–1951 calBC (3655±20 BP, PSUAMS-2318)	De Tuithoorn, Oostwoud, Noord-Holland	The Netherlands
I4076	1882–1750 calBC (3490±20 BP, PSUAMS-2319)	De Tuithoorn, Oostwoud, Noord-Holland	The Netherlands
I4075	2118–1937 calBC (3635±20 BP, PSUAMS-2337)	De Tuithoorn, Oostwoud, Noord-Holland	The Netherlands